(2)

NASA
Contractor Report 185110

AVSCOM
Technical Memorandum 89-C-003

AD-A216 002

Two Stage Gear Tooth Dynamics Program

Linda S. Boyd
Hamilton Standard Division
United Technologies Corporation
Windsor Locks, Connecticut

August 1989

Prepared for
Lewis Research Center
Under Contract NAS3-25281

NASA
National Aeronautics and Space Administration

US ARMY
AVIATION
SYSTEMS COMMAND
AVIATION R&T ACTIVITY

Foreword

The author would like to acknowledge the assistance of the Technical Manager, J. Zakrajsek of NASA Lewis, and W. Westervelt of Hamilton Standard, Division of United Technologies.

Table of Contents

I. Summary

The purpose of this contract was to expand the epicyclic gear dynamics program to add the option of evaluating the tooth pair dynamics for two epicyclic gear stages with peripheral components. The option was developed for either stage to be a basic planetary, star, single external-external mesh, or single external-internal mesh. The two stage system includes an input mass and shaft, an output mass and shaft, and a connecting shaft, where the shafts are each modeled with torsional springs and dampers. The solution procedure was nearly the same as the procedure previously used for determining tooth pair displacements and stresses in single stages. The primary differences were that the individual gear component displacements were calculated rather than the net sun-planet or ring-planet displacements. This was necessary in order to determine the relative displacements between the shafts and the input and output gears. This generally increases the number of degrees of freedom to be solved per stage compared to the single stage solution.

The option to evaluate two stages makes the user's job more difficult. Two stages of basic gear system information must be input as well as the additional component information. In addition, the boundary conditions and associated iteration procedure become more complex. This is due to both the increased number of components and to the time for a complete mesh generally being different for each stage.

A brief investigation into methods of reducing the program's computation time was done. The efforts focused on reducing the number of iterations required for boundary condition convergence. It was recommended that the beginning and ending values be weighted differently to utilize previous iterations more effectively. As over 90% of the computation time is in the numerical integration routines, reducing the number of solution integrations would yield a direct, linear reduction in time.

Execution of the initial test case indicated an instability in the solution. The tooth pair load pattern is reasonable however the magnitudes of the tooth pair loads grow to excessive, unrealistic values as a function of time. This could be due to the initial conditions, a code error, or some type of numerical instability. A procedure has been recommended for eliminating possibilities and determining where the problem lies.

II. Introduction

Over the past several years, NASA nas developed a gear dynamic analysis and computer code for standard and high contact ratio gears. The analysis was expanded to include internal involute tooth forms in addition to external involute tooth forms, then expanded to include several planets in epicyclic gear systems. The development continued with the addition of helical and double helical gears, a floating sun gear option, a natural frequency evaluation, a refined helical gear compliance routine, and a flexible carrier evaluation.

The initial program was developed for a single spur gear mesh and to operate over a wide range of contact ratios (up to 4.0) for analysis of high contact ratio as well as low contact ratio gearing. This single mesh program was an extension, by Cornell and Westervelt (references 1 and 2), of the basic concept developed by Richardson in 1958 (reference 3). The tooth pair compliance and stress sensitivity formulation of the single spur gear mesh program was used in the epicyclic gear dynamics program, applied to each mesh.

This contract, NAS3-25281, developed an option for two spur gear stages with input and output shafts with attached masses and a shaft connecting the two stages. This was a practical extension to the program as more than one gearing stage are often used for speed reduction, space, weight, and/or auxiliary units. Thus, this extension allows for modeling of peripheral components in order to assess the impact on the gear tooth stressing. Although the basic code was completed, the cause of the unexpected instability in the results could not be determined with the cost constraints of the contract. NASA, therefore, decided to accept delivery of the code and documentation rather than extend the contract at this time.

III. Task I-Multiple Gearing Stages and System Components

The first two tasks of contract NAS3-25821 were to modify the existing Multi-Mesh Gear Dynamic Analysis Code (GEARDYNMULT in NASA notation, F178 in Hamilton Standard notation) to include a second stage and peripheral components. These tasks included the technical development and most of the coding efforts. Another smaller task was to investigate methods of reducing computation time.

A. Analytical Model

The dynamic response equations for a single gear stage were expanded to include additional degrees of freedom for an input shaft and attached input mass, and an output shaft with an output mass. This was accomplished by adding two new equations and modifying other equations. Figure 1 shows a diagram of the two stage system with no details for the individual gear stages. Figure 2 shows a general schematic for either epicyclic gear stage. The specifics of the gear tooth dynamics and program capabilities for each stage are discussed in References 1-7.

For the numerical model, the input and output shafts each required an additional second order differential equation to account for the inertias on the input and output shafts.

The equation for the input shaft and attached mass is:

$$J_{in}\,\ddot{\theta}_{insh} + C_{in}(\dot{\theta}_{insh} - \dot{\theta}_{in1}) + k_{in}(\theta_{insh} - \theta_{in1}) = \tau_{in} \qquad (1)$$

where $\theta_{in1} = \dfrac{Y_{\text{input gear for stage 1}}}{\text{base radius of the input gear to stage 1}}$

The equation for the output shaft and attached mass is:

$$J_{out}\,\ddot{\theta}_{outsh} + C_{out}(\dot{\theta}_{outsh} - \dot{\theta}_{out2}) + k_{out}(\theta_{outsh} - \theta_{out2}) = \tau_{out} \qquad (2)$$

The addition of these equations changes the way the torque is fed into and out of the individual stages. Previously, there was a constant input torque term in the sun gear equation and a constant output torque term in either the ring or carrier equation. The torque is now fed into the input gear equations by way of shaft rotational displacements and velocities, which vary with time. The rotational displacements are transformed into equivalent displacements along the line of action for each mesh of the input gear. The output gear equations also have the

equivalent shaft displacement and velocity terms in place of the output torque terms.

The new two stage program has the capability of solving for the dynamic tooth loads in planetary systems, star systems , single mesh external-external involute tooth forms, and/or single mesh external-internal involute systems. Table 1 summarizes the available spur gear systems for two stage dynamic solutions. The two stage program has been expanded to allow the user to specify the input and output gears The single stage solution assumed the systems were speed reduction systems, but the two stage solution also allows for speed increasing systems. This option will allow the user to model a back-to-back test rig, which is generally one reduction system and a second similar system which increases the speed. For example, a single stage planetary system normally has the sun gear as the input and the planet carrier for the output. For the two stage solution, the planetary system can have the input component as either the sun gear or the carrier with the output being either the carrier or the sun gear respectively.

The equations for each separate gear component were the same as previously developed. The basic equation development was documented in References 4-7, and the equations are summarized in Appendix A for convenience. The input and output gears for each stage will depend on the specified system type, see Table 1. Thus, the additional terms needed in the gear equations, due to the shafting, are written in terms of general input and output gear equations, and are as follows.

input gear equation for stage 1

$$+ C_{in} (\dot{Y}_{in1} - \dot{Y}_{insh}) + k_{in} (Y_{in1} - Y_{insh}) = 0 \qquad (3)$$

output gear equation for stage 1

$$+ C_{12} (\dot{Y}_{out1} - \dot{Y}_{in2}) + k_{12} (Y_{out1} - Y_{in2}) = 0 \qquad (4)$$

input gear equation for stage 2

$$+ C_{12} (\dot{Y}_{in2} - \dot{Y}_{out1}) + k_{12} (Y_{in2} - Y_{out1}) = 0 \qquad (5)$$

output gear equation for stage 2

$$+ C_{out} (\dot{Y}_{out2} - \dot{Y}_{outsh}) + k_{out} (Y_{out2} - Y_{outsh}) = 0 \qquad (6)$$

where: $Y_{insh} = (R_b$, input gear to stage 1$)\ \theta_{insh}$

$Y_{outsh} = (R_b$, output gear from stage 2$)\ \theta_{outsh}$

Transformations from shaft rotations to displacements along the appropriate line of action are necessary to determine the tooth pair displacements along the line of action. This allows the tooth pair displacements and loads to be determined by a procedure similar to the single stage procedure.

The numerical solution of the dynamic equations utilizes IMSL (International Mathematic and Scientific Library) numerical integration routines. These routines solve a system of first order differential equations. Appendix B shows the reduction of the second order equations to first order equations.

The tooth pair displacements along the line of action are calculated from the gear component displacements via:

$$Y_{sp} = Y_s - Y_c - Y_{pi} \tag{7}$$

$$Y_{rp} = Y_{pi} - Y_c - Y_r \tag{8}$$

For the single stage solution, the generalized coordinates to be solved by the numerical solution were the tooth pair displacements along the line of action (Y_{sp} and Y_{rp}), which minimized the number of equations to be numerically solved. For the two stage system of equations, the individual gear component equations must be solved. This was necessary in order to obtain the input and output gear displacements (Y_s, Y_r, Y_c, Y_{pi}) for both stages. Therefore the relative displacement terms between the shafts and the input or output gears could be calculated. This means there are more degrees of freedom to be solved for each stage in the two stage solution . There are (3 + number of planets) degrees of freedom for each stage plus two degrees of freedom for the input and output shafts. Thus, there are a total of $(8 + N_1 + N_2)$ second order equations and $2(8 + N_1 + N_2)$ first order equations to be solved simultaneously.

The input and output shaft damping terms are calculated from a damping ratio, stiffness, and inertias. The damping coefficients are then calculated using the following formulations.

$$C_{in} = 2\,\xi\,[k_{in}/\,(\,1/J_{in} + 1/J_{in1}\,)\,]^{1/2} \tag{9}$$

$$C_{out} = 2\,\xi\,[k_{out}/\,(\,1/J_{out} + 1/J_{out1}\,)\,]^{1/2} \tag{10}$$

$$C_{12} = 2\,\xi\,[k_{12}/\,(\,1/J_{out1} + 1/J_{in2}\,)\,]^{1/2} \tag{11}$$

B. Solution Procedure

The solution procedure used to determine the two stage dynamic gear tooth loads and stresses was very similar to the solution for the single stage dynamic gear tooth loads and stresses. To minimize the program modifications, as many of the existing methods and procedures as possible were used. Most sections of the program needed some modification in order to process the additional stage. Many of the slightly modified routines were used twice, once for each stage, by sending the necessary information for the relevant stage.

The single stage solution procedure will be reviewed first, because the two stage solution procedure is essentially an extension of the single stage procedure. The general program procedure is illustrated via a flowchart in Figure 3. In brief, the program calculates tooth pair loads and solves the differential equations for each of 100 time steps--a piecewise linear solution. The boundary conditions are determined via an iterative procedure, which will be explained in more detail later.

The boundary condition iteration procedure is intended to lead to a steady state condition. For the single mesh this is accomplished by evaluating one full mesh cycle, where a mesh cycle means the time required for a tooth pair to move the length of the line of action. The mesh cycle time for spur gears is divided into 100 time steps for the numerical time stepping solution, where each increment of time is treated as linear with respect to the tooth pair stiffnesses. The boundary conditions, for sun-planet and ring-planet tooth pair displacements and velocities, are compared at the beginning and end of the mesh time cycle. If the displacements and velocities are within a specified tolerance, the system has reached a steady state. If the conditions are not within the tolerance the initial and final values of the displacements and velocities are averaged to obtain a new set of initial conditions, and the procedure is repeated with new initial conditions. This procedure is repeated until the boundary conditions are all within the specified tolerance. The final iterated 100 time step solution for tooth pair loads and displacements is then post-processed for tooth stressing.

The boundary conditions for two stages become quite complex compared to one stage. The main complexity is due to the two stages having different mesh time cycles. This means that steady state is no longer achieved for one mesh cycle, rather it must be a mutually common time for both stages, analogous to a common denominator. Figure 4 schematically shows two examples. The first one shows a case where the two stages have time cycles that can readily achieve a steady state, i.e. one stage has a time cycle exactly 2 times the other stage's time cycle. The other example shows a case where 47 cycles would have to be evaluated for steady state, which would consume large quantities of computer time (and a code change to increase the size of an array). However, it is thought that this case could be approximated by evaluating five cycles. It follows that there are systems in which there is no true steady state.

Once the boundary conditions have converged, the tooth pair steady state displacements are post-processed for stressing through the 100 time steps. If any tooth pair errors have been requested for evaluation, the program continues to evaluate 10 time cycles to simulate the user input tooth pair errors going through a mesh for either one or two stages. The method used to process the tooth pair errors starts with the converged boundary conditions from the no tooth errors solution as the initial conditions for the numerical solution with errors. The program thus simulates a transient response (for a duration of ten mesh cycles) as the various tooth pair errors come into mesh. The dynamic effects of the tooth pair errors have generally been observed to dampen out after evaluation of 3-5 mesh cycles.

For the two stage expansion, it was desirable to work with the current procedure to maintain commonality. This implied that the 100 time steps, corresponding to a mesh cycle time, needed to be maintained, as this fundamental approach is used throughout the program. The first question was which stage's time cycle should be used to correspond to the 100 time steps embedded in the program. A smaller time step for the numerical solution would tend to make for a more stable numerical solution, while the larger time step would reduce the computation time. The smaller time step was chosen for stability reasons.

The other question was how to handle the two different mesh times in order to achieve a "steady state" in a practical amount of computation time. It was decided that the program could be set up to evaluate the boundary conditions after a user specified number of time cycles was evaluated. However, the fact that there could be cases with no true steady state made it desirable to try and approximate a steady state and then evaluate a transient response using the approximated boundary conditions as initial conditions. It is possible that the instability could be related to these approximate steady state boundary conditions.

In order to verify the approximate steady state boundary condition concept, the original single mesh program was used to determine if a small change in the mesh time cycle would significantly affect the converged boundary condition values. Several cases were run with slightly different numbers of teeth (which determines the mesh time). The iterated results showed minimal variation in the converged values for displacement and velocity. Thus, this implied that it would be possible to evaluate 'approximate two stage boundary conditions' at a time when the two stages were close to a steady state. The program will use the initial conditions obtained from the approximate steady state solution and continue to evaluate 10 additional cycles for a transient response. The transient response utilizes the same procedure used to evaluate tooth pair errors in the single stage code. The solution procedure, with 100 time steps per cycle, is essentially the same except there is no boundary condition averaging. It should be noted that the two stage solution compares the tooth pair displacements and velocities for convergence, not the individual gear components. The initial and final conditions for the individual components are each averaged and that average is used for the initial conditions for the next iteration.

The subroutines written for the two stage solution generally follow similar notation to that used in previous codes, both in subroutine names and variable names. The code was written assuming a maximum of 10 planets per stage, spur gears only, and no floating sun or flexible carrier option.

Several new routines and some slightly modified routines were written in order to accommodate the additional information required for two different stages. The number of planets per stage is limited to 10, which should be more than sufficient for any real system. This is a reduction in the number of planets allowed in the single stage solution, but simplifies the code changes by utilizing the existing arrays and the corresponding dimensions. The arrays now contain stage 1 information in the first 10 elements and stage 2 information in the second 10 elements, for the same total number of array elements as the previous solution.

The procedures and calculations of the new program are essentially the same as the single stage program. The primary changes come through nearly every section or subroutine being executed for stage 1 and then for stage 2. Some of the basic parameters, such as mesh time cycle, required additional logic in order to implement the option of "reversed" systems (where the systems are speed increasers rather than reducers). Most of the minor modifications were made to accommodate the additional parameters of the second stage, and did not change any basic concepts. Because of the option of multiple cycles being evaluated for boundary condition convergence, it was also necessary to add a dummy time parameter to obtain proper tooth pair contact. Without the dummy time parameter, the stage with the shorter mesh time cycle lost all tooth pair contact during the second 100 time steps. Thus, to obtain proper contact evaluation, a dummy time was reset to zero at the beginning of each mesh time cycle for the stage with the smaller mesh time cycle.

The input routines were modified to meet NASA programming standards. The additional stage of information necessary for the two stage solution required modification of the code to set up the input variables. This portion of the code was previously in the preprocessing routine; however, the preprocessing routine (READ2) is a very large routine and does not meet the 150 executable line requirement. Thus, the section of the code for setting input variables to meaningful notation was modified to be separate subroutines, accepting input for either one or two stages of information, and the remainder of READ2 remained unchanged except for additional arguments. Three subroutines were necessary to convert a section of the old routine into acceptable length routines and a fourth was necessary to control which stage was being preprocessed.

C Methods of Reducing Computation Time

Part of Task I was to recommend a method for possible future development work in "alternate methods for expanding the model to more than two stages (such as a superposition dynamic model)." The stated reason for such a recommendation was the potential for extensive computational times.

The approach to this task was to emphasize the reduction in computer time required by the program. In analyzing the present CPU usage of the program, it was determined that over 90 percent of the computational time was in the numerical integration routine. The basic alternatives to reducing program solution time were as follows.

a. Reduce the number of time steps used through the mesh for a direct, linear reduction in time.

b. A more advanced solver routine for an unknown time reduction.

c. Reduce the number of iterations required for boundary condition convergence for a direct linear reduction in time.

Item a. was thought to be practical for single mesh cases only, since only in these cases could the timing of events through the mesh time cycle, be accurately estimated. Item b. was not thoroughly explored, but was felt to hold some promise. Item c. was the main focus of this study, and could be applicable to any level of the code, i.e., single mesh, multiple mesh, and multiple stages.

In order to investigate better methods of convergence, the flexible barrier test case given in Reference 4 was used. This case was initially solved by calculating input conditions as specified in Appendix A of Reference 4, and many boundary condition iterations, which use significant CPU time.

Figure 5 is a plot of the ending values of the sun gear displacement and velocity versus the number of iterations through a gear mesh period. It shows that the method of selecting new values is creating a cyclic behavior that will take many iterations to converge. The mean value of the plotted functions match the converged value of the solution. The behavior of the planet and ring gear results was similar.

In order to evaluate the convergence difficulties, the code was temporarily changed to weigh the beginning and ending values differently in order to obtain a higher weighting to previous iterations. The revised code, shown in Figure 6, has not been incorporated in the new program, but was used for this investigation only. The convergence could be tailored for a particular case by changing coefficients of the displacements from the previous iteration and the current iteration (e.g. .XIN5 and .X55 respectively), and similarly for the velocities (SXS1 and .XI1). The sum of the coefficients must be equal to unity. The results of using 0.7 and 0.3 for the displacement, and 0.5 and 0.5 for the velocity are shown in Figures 7 and 8.

In order to reduce the computation time for a dynamic solution, it is recommended that this method be added to the code, with the weighting coefficients as input parameters rather than fixed values in the code. It is further recommended that code be written to automate the plots as shown in Figures 7 and 8. The resulting code should substantially enhance the user's understanding and the convergence of the boundary conditions.

D. Discussion of Instability and Test Cases

Task Ic was to evaluate the two stage model and determine the interaction between two stages and the effects of input and output shafting and attached masses. This was not fully accomplished due to the initial test case showing an instability in the results. However, some general comments will be made regarding the apparent instability and other observations from a variety of test cases.

The first test case that was used approximated the OH-58 dropped tooth planetary design being tested at NASA Lewis. A dropped tooth design "drops" a tooth from each of the planets so that the number of teeth on a planet divided by the number of planets is not an integer number. The purpose of the design is to reduce dynamic tooth loading. The actual planetary system could not be modeled with the program, because the dropped tooth design leads to different pressure angles for the sun-planet and ring-planet meshes. The program assumes equal pressure angles for the sun-planet and ring-planet mesh, although an equivalent buttress tooth form might be a feasible modeling method. Figure 9a shows the input test case for a single stage and Figure 9b shows the corresponding output summary. This case had assumed the pressure angle of the sun-planet mesh for both the sun-planet and ring-planet meshes and used the program's geometry preprocessor.

The next step was to evaluate two stages, simulating the back-to-back test rig at NASA. An example input data set for two stages is shown in Figure 10. The first stage was modeled as a planetary, with the sun gear as the input gear, and the second stage was a "reversed planetary" with the carrier as the input. This case was used for initial verification of the code interaction and debugging purposes. The geometry for the two stages was the same, with the primary difference between the stages being the input torque and rpm. The different torques led to slightly different tooth pair stiffnesses, as the torque level influences the Hertzian component of the stiffness function, see reference 2. The difference in rpm could affect the dynamic load levels, particularly if near a resonant speed.

Table 3 summarizes the test cases run with the two stage program and the resulting component displacements. The initial test case, case 1, was designed to uncouple stage 1 from stage 2. Thus, the connecting shaft stiffness was very low. The input and output shaft stiffnesses were also low, because some preliminary test case results indicated large displacements for very stiff input and output shafts. The solution seemed to be very sensitive to the values of the shaft stiff-

nesses, as indicated by comparison of case 4 and 5 (stage 1). For a decrease in input shaft stiffness by a factor of ten, the magnitudes of the planetary component displacements along the line of action decreased by orders of magnitude.

Some of the dynamic load results for the initial test case have been plotted in Figure 11. These results illustrate a typical tooth pair meshing pattern of engagement and disengagement of the teeth. The meshing pattern also repeats for subsequent cycles, as would be expected. What is unusual about these test results, is the substantial increase in the magnitude of the loads as time progresses. This increasing magnitude is also illustrated in Figure 12, which shows the maximum stress in a cycle vs. the transient cycle number. It is evident from this figure that there is some type of instability in the solution. It is interesting that the Hertz stress increases in a nearly linear fashion, while the maximum bending stress is a higher order function. This is logical in that a nonlinear increase in loads would correspond to a nonlinear increase in bending stress. It is recommended that the system equations be evaluated for stability.

The cases summarized in Table 3 show the effect of varying the input and output masses and shaft stiffnesses. Only one boundary condition iteration was performed, which was sufficient to observe the change in the component displacements due to the modified parameter(s). The affect of varying the masses on the input or output shaft was inversely proportional to the input or output shaft displacements respectively. For example, the input mass for case 2 is 10 times the input mass for case 1 and the input shaft rotational displacement decreased by the same factor of 10. The other stage 1 component displacements, sun, carrier, and planets, also showed decreases of nearly the same factor. This indicates that the shaft displacements are dominating the individual input and output gear equations, and the tooth pair dynamics are therefore overshadowed.

Case 3 is the same as Case 1 except the input and output masses have been reversed. The input and output shaft displacements were correspondingly interchanged. As would be expected, the gear displacements for the two stages were interchanged also, but with some variation due to the change in torque and rpm of the two stages.

In Case 4, a very stiff shaft connecting the two stages was investigated. This case verified that the displacement of the output gear from Stage 1 (planet carrier) would equal the displacement of the input gear to Stage 2 (planet carrier) for a rigid connection.

Case 5 was a check case to verify that the input mass and shaft could be isolated from Stage 1 by using zero torsional shaft stiffness. By using a low connecting shaft stiffness, this case also verified that the two stages could be isolated from each other. By having zero torsional input shaft stiffness, there is no torque transmitted to the input gear of Stage 1 and therefore approximately zero displacements in Stage 1. The second stage displacements were nearly the same as Case 4, which verified the stages were isolated from each other.

Case 6 was nearly the same as Case 4, but the connecting shaft stiffness was a lower and more realistic value. All of the component displacements were slightly larger for the softer shaft. There was also a small difference in the magnitudes of the output gear from Stage 1 and the input gear to Stage 1. This is logical, because as the connecting shaft stiffness decreases, the relative displacement of the two ends will increase.

Case 7 increased the torsional stiffness of the input shaft by several orders of magnitude. The resulting displacements shown in Table 4 indicate the displacements also increased by orders of magnitude for the first stage components. The second stage component displacements also increased substantially, but not as much as the first stage.

There are several possibilities for the source of the instability. Figure 13 illustrates a procedure for eliminating possibilities and tracking down the problem. The recommended procedure would start with a very simple "two stage" system, as shown schematically in Figure 14. This simple system, effectively a gear train, with constant tooth pair stiffnesses could be evaluated using a small program, separate from the gear program. The system should have a 1:1 gear ratio for simplicity and to ensure a steady state can be achieved for boundary condition convergence. If the simple system shows an unstable behavior, it will be known that there is a problem with the basic problem formulation. That is the least likely source of the problem, but it is the logical starting point. The model complexity can then be increased by adding in the variable tooth pair stiffness. If the independent solution yields reasonable results, the same system can be run in the full multiple mesh gear program. If the results are inconsistent, it would indicate an error in the two stage multiple mesh code.

If the results are consistent for the 1:1 gear ratio cases, the problem is most likely related to the initial conditions and/or the boundary condition iteration scheme. This would indicate a better method for estimating the initial conditions and for determining convergence should be devised. It should be noted that this is not minor task. In general, each stage plus an input or output shaft will have 2 times (4 + number of planets) for boundary conditions to be determined. Not only is it difficult to obtain initial estimates for the tooth displacements and velocities for each component of the epicyclic stage, but it is even more difficult to determine a general method of combining the two stages.

Another test case was tried to determine if the instability was system dependant. The second case chosen was the Stoeckicht 2K-H planetary from Reference 5. The two stage test case was set up as two planetary reduction stages with identical geometry and basic gear parameters. The only difference between these two stages would be the torque and the rpm. This case exhibited similar instabilities, with tooth loads increasing substantially with time.

IV. Concluding Remarks

An option to evaluate two gear stages, with a connecting shaft and input and output shafts with attached masses, has been added to the epicyclic gear tooth dynamic analysis program. There were extensive code modifications to accommodate two stages of: geometry preprocessing, tooth pair load calculations, and dynamic equations. The new code utilizes the same general methods and procedures as were previously used for the single stage solution and includes additional degrees of freedom for the attached masses. The two stage option also allows for speed increasing systems as well as speed reduction systems.

It is recommended that code changes be incorporated for a more robust boundary condition iteration scheme. The proposed code changes can significantly reduce the number of iterations required for a converged steady state solution, and therefore reduce the computation time for a dynamic solution.

The program's plotting capabilities should be modified to use more universal plotting routines. The plotting capabilities should also be expanded to process the large amount of output from a two stage solution. In addition, plotting capabilities for the boundary conditions should be added to enhance the user's understanding of the boundary condition convergence process.

The initial test case indicated an instability in the dynamic solution, where the gear tooth displacements continually increase with time, beyond any reasonable values. Several variations on shaft stiffnesses, attached masses and shaft damping were evaluated to investigate the problem. The tooth pair loads with respect to time indicated the tooth pair contact patterns were reasonable, in that the basic pattern was repeated with time, although the magnitudes continued to increase. Further evaluation of the problem could not be made because of fund limitations.

V. References

1. R.W. Cornell, and W.W. Westervelt, "Dynamic Tooth Loads and Stressing for High Contact Ratio Spur Gears", Journal of Mechanical Design, January 1978.

2. R.W. Cornell, "Compliance and Stress Sensitivity of Spur Gear Teeth", Journal of Mechanical Design, April 1981, Vol. 103.

3. H.H. Richardson, "Static and Dynamic Load, Stresses, and Deflection Cycles in Spur-Gear Systems", Sc.D. Thesis; MIT Report, 1958.

4. L. S. Boyd and J. A. Pike, "Expansion of Epicyclic Gear Dynamic Analysis Program", NASA CR-179563, August 1986.

5. L.S. Boyd and J.A. Pike, "Multi-Mesh Gear Dynamics Program Evaluation and Enhancements", NASA CR-174747, September 1984.

6. J.A. Pike, "Interactive Multiple Spur Gear Mesh Dynamic Load Program", NASA CR-165514, December 1981.

7. J.A. Pike, "Expansion of the Dynamic Load solution for Multiple Planet Spur Gearing to Helical Gearing", Documentation Report to NASA Lewis, September 1983.

Appendix A. Epicyclic Gear System Equations for Either Stage

The following second order equations of motion describe the individual gear components in an epicyclic system. They are written in terms of the displacements along the lines of action. The development of the basic equations is documented primarily in Reference 1 and 6.

Sun gear equation:

$$m_s \ddot{y}_s + \sum_{i=1}^{N} d_{sp_i} \dot{y}_{sp_i} + \sum_{i=1}^{N} L_{sp_i} = \tau_{in_s} / R_{b_s} \qquad (A.1)$$

Planet gear equation:

$$m_{p_i} \ddot{y}_{p_i} - d_{sp_i} \dot{y}_{sp_i} + d_{rp_i} \dot{y}_{rp_i} - L_{sp_i} + L_{rp_i} = 0 \qquad (A.2)$$

Ring gear equation:

$$m_r \ddot{y}_r - \sum_{i=1}^{N} d_{rp_i} \dot{y}_{rp_i} - \sum_{i=1}^{N} L_{rp_i} = \tau_{out} / R_{b_r} \qquad (A.3)$$

Carrier equation:

$$m_c \ddot{y}_c - \sum_{i=1}^{N} d_{rp_i} \dot{y}_{rp_i} - \sum_{i=1}^{N} d_{sp_i} \dot{y}_{sp_i} - \sum_{i=1}^{N} L_{rp_i} - \sum_{i=1}^{N} L_{sp_i} = \tau_{out} / R_{b_c} \qquad (A.4)$$

NOTE: For the two stage solution, the constant torque terms indicated above go to zero. The "torque" is input to the appropriate gear equations via terms for relative displacement with respect to a shaft.

The tooth pair load terms are determined from the following equations.

$$L_{sp_i} = \sum_{j=1}^{m} [(y_{sp_i} - e_{sp_{ji}} - \chi^2_{sp_{ji}} \beta^2_{sp_{ji}}) \eta_{sp_{ji}} \phi_{sp_{ji}}] \qquad (A.5)$$

$$L_{rp_i} = \sum_{j=1}^{m} [(y_{rp_i} - e_{rp_{ji}} - \chi^2_{rp_{ji}} \beta^2_{rp_{ji}}) \eta_{rp_{ji}} \phi_{rp_{ji}}] \qquad (A.6)$$

Appendix B: First Order Differential Equations

The numerical integration routines solve for a system of first order equations. The transformation of the second order differential equations to first order equations is shown below. The subscripted numbers on the derivatives correspond to elements in the array (X1) in the program.

Input shaft equation reduction:

Let

$$\dot{x}_3 = \ddot{\theta}_{insh} \tag{B.1}$$

$$\dot{x}_4 = x_3 = \dot{\theta}_{insh} \tag{B.2}$$

Then

$$\dot{x}_3 = [\ \tau_{in} - C_{in}(\dot{x}_4 - \dot{\theta}_{in1}) - k_{in}(x_4 - \theta_{in1})]/J_{in} \tag{B.3}$$

$$\dot{x}_4 = x_3 \tag{B.4}$$

Output shaft equation reduction:

Let

$$\dot{x}_5 = \ddot{\theta}_{outsh} \tag{B.5}$$

$$\dot{x}_6 = x_5 = \dot{\theta}_{outsh} \tag{B.6}$$

Then

$$\dot{x}_5 = [\ \tau_{out} - C_{out}(\dot{x}_6 - \dot{\theta}_{out2}) - k_{out}(x_6 - \theta_{out2})]/J_{out} \tag{B.7}$$

$$\dot{x}_6 = x_5 \tag{B.8}$$

The remaining equations will vary depending on the specific system type, see table of system types in the main report text. For simplicity, the following first order equation derivations will assume both stage 1 and stage 2 are planetary systems. Thus, the generalized input and output gear equations in equations 3 - 6 are now specified, where the input gear is the sun gear and the output gear is the planet carrier for both stages.

Sun gear equation for stage 1:

Let

$$\dot{x}_1 = \ddot{Y}_S = \ddot{\theta}_{in1}\, R_{bs} \tag{B.9}$$

$$\dot{x}_2 = x_1 = \dot{Y}_S \tag{B.10}$$

Then

$$\dot{x}_1 = -\left[\sum_{i=1}^{N1} d_{sp_i}\dot{y}_{sp_i} + \sum_{i=1}^{N1} L_{sp_i} + C_{in}(\dot{x}_2 - R_{bs}\dot{x}_4) + k_{in}(x_2 - R_{bs}x_4)\right] / m_s \quad \text{(B.11)}$$

$$\dot{x}_2 = x_1 \quad \text{(B.12)}$$

Carrier equation for stage 1:

Let

$$\dot{x}_7 = \ddot{y}_c \quad \text{(B.13)}$$

$$\dot{x}_8 = x_7 = \dot{y}_c \quad \text{(B.14)}$$

Then

$$\dot{x}_7 = \left[\sum_{i=1}^{N1} d_{rp_i}\dot{y}_{rp_i} + \sum_{i=1}^{N1} d_{sp_i}\dot{y}_{sp_i} + \sum_{i=1}^{N1} L_{sp_i} + \sum_{i=1}^{N1} L_{rp_i} - C_{12}(\dot{x}_8 - \dot{x}_{12}) - k_{12}(x_8 - x_{12})\right] / m_c \quad \text{(B.15)}$$

$$\dot{x}_8 = x_7 \quad \text{(B.16)}$$

Ring gear equation for stage 1:

$$\dot{x}_9 = \ddot{y}_r = 0.0 \quad \text{(B.17)}$$

$$\dot{x}_{10} = x_9 = \dot{y}_r = 0.0 \quad \text{(B.18)}$$

Note: ring gear is fixed for a planetary system.

Planet gear equations for stage 1:

Let

$$\dot{x}_{i+16} = \ddot{y}_{pi} \qquad \text{for } i = 1 \text{ to } N1 \quad \text{(B.19)}$$

$$\dot{x}_{i+N1+16} = \dot{x}_{i+16} \qquad \text{for } i = 1 \text{ to } N1 \quad \text{(B.20)}$$

Then

$$\dot{x}_{i+16} = \left[d_{sp_i}\dot{y}_{sp_i} - d_{rp_i}\dot{y}_{rp_i} + L_{sp_i} - L_{rp_i}\right] / m_{p_i} \quad \text{(B.21)}$$

$$\dot{x}_{i+N1+16} = x_{i+16} \quad \text{(B.22)}$$

Sun gear equation for stage 2:

Let

$$\dot{x}_{11} = \ddot{Y}_{s2} \tag{B.23}$$

$$\dot{x}_{12} = x_{11} = \dot{Y}_{s2} \tag{B.24}$$

Then

$$\dot{x}_{11} = -\left[\sum_{i=1}^{N2} d_{sp2_i} \dot{Y}_{sp2_i} + \sum_{i=1}^{N2} L_{sp2_i} + C_{12}(\dot{x}_{12} - \dot{x}_8) + k_{12}(x_{12} - x_8) \right] / m_{s2} \tag{B.25}$$

$$\dot{x}_{12} = x_{11} \tag{B.26}$$

Carrier equation for stage 2:

Let

$$\dot{x}_{13} = \ddot{Y}_{c2} = \ddot{\theta}_{out2} R_{bc2} \tag{B.27}$$

$$\dot{x}_{14} = x_{13} = Y_{c2} \tag{B.28}$$

Then

$$\dot{x}_{13} = \left[\sum_{i=1}^{N2} d_{rp2_i} \dot{Y}_{rp2_i} + \sum_{i=1}^{N2} d_{sp2_i} \dot{Y}_{sp2_i} + \sum_{i=1}^{N2} L_{sp2_i} + \sum_{i=1}^{N2} L_{rp2_i} - C_{out}(R_{bc2}\dot{x}_6 - \dot{x}_{14}) - k_{out}(R_{bc2}x_6 - x_{14}) \right] / m_{c2} \tag{B.29}$$

$$\dot{x}_{14} = x_{13} \tag{B.30}$$

Ring gear equation for stage 2:

$$\dot{x}_{15} = 0.0 \tag{B.31}$$

$$\dot{x}_{16} = x_{15} = \dot{Y}_{r2} = 0.0 \tag{B.32}$$

Note: ring gear is fixed for a planetary system.

Planet gear equations for stage 2:

Let

$$\dot{x}_{i+2N1+16} = \ddot{x}_{pi} \qquad \text{for } i = 1 \text{ to } N2 \tag{B.33}$$

$$\dot{x}_{i+2N1+N2+16} = x_{i+2N1+16} \tag{B.34}$$

$$\dot{x}_{i+2N1+16} = \left[d_{sp2_i} \dot{y}_{sp2_i} - d_{rp2_i} \dot{y}_{rp2_i} + L_{sp2_i} - L_{rp2_i} \right] / m_{p2_i} \tag{B.35}$$

$$\dot{x}_{i+2N1+N2+16} = x_{i+2N1+16} \tag{B.36}$$

Appendix C. Nomenclature

C_{in} = damping coefficient for the input shaft (in-lbs-s/rad)

C_{out} = damping coefficient for the output shaft (in-lbs-s/rad)

C_{12} = damping coefficient for the output shaft (in-lbs-s/rad)

d_{rp_i}, d_{sp_i} = tooth pair damping (lb-s/in)

$e_{rp_{ij}}$, $e_{sp_{ij}}$ = tooth spacing error (in)

J_{in} = rotational inertia attached to input shaft (in-lbs-s^2/rad)

J_{out} = rotational inertia attached to output shaft (in-lbs-s^2/rad)

k_{in} = torsional stiffness of the input shaft (in-lb/rad)

k_{out} = torsional stiffness of the output shaft (in-lb/rad)

k_{12} = torsional stiffness of the shaft connecting the two stages

L_{rp_i}, L_{sp_i} = tooth pair loads for planet mesh i (lbs)

m = rotational (equivalent) mass (lb-s^2/in)

N = number of planets

R = base radius (in)

Y = displacement along the line of action (in)

$\delta_{rp_{ji}}$ = cam modification, ring-planet mesh

$\delta_{sp_{ji}}$ = cam modification, sun-planet mesh

γ_{rp_i} = ring-planet tooth pair spring rates

γ_{sp_i} = sun-planet tooth pair spring rates

θ = rotational displacement (rad)

ξ = damping ratio

τ_{in} = input torque (in-lb)

τ_{out} = output torque (in-lb)

$\phi_{rp_{ji}}$ = identity function for ring-planet tooth pair contact

$\phi_{sp_{ji}}$ = identity function for sun-planet tooth pair contact

χ_{sp} = 0 or 1 depending on whether the tooth contact is on the profile modification cam or not

Subscripts

insh = input shaft

outsh = output shaft

in1 = input gear to stage 1

in2 = input gear to stage 2

out1 = output shaft from stage 1

out2 = output shaft from stage 2

in = Regarding input

out = Regarding output shaft

s = sun gear

pi = planet gear i

r = ring gear

c = carrier

sp = sun planet mesh

rp = ring planet mesh

12 = shaft connecting stage 1 to stage 2

1 = stage 1

2 = stage 2

Table 1: Spur Gear Systems Available for Two Stage Dynamic Solution

System number	Spur Gear System Type	Input Gear	Output Gear
1	planetary system	sun gear	planet carrier
-1	planetary system	planet carrier	sun gear
2	star system	sun gear	ring gear
-2	star system	ring gear	sun gear
4	single external-external* mesh	sun gear	planet gear
-4	single external-external* mesh	planet gear	sun gear
5	single external-internal** mesh	planet gear	ring gear
-5	single external-internal** mesh	ring gear	planet gear

* External-external mesh means a pinion and a gear, both with external involute tooth forms.

** External-internal mesh means a pinion and a gear, with the pinion having an external involute tooth form and the gear having an internal tooth form.

Table 2: OH-58 Planetary Characteristics

System Type:	Planetary
Speed Range:	Up to 1620 rpm (sun gear)
Torque Range:	Up to 12,450 in-lb (sun gear)
Number of Planets:	3
Stage 1 input:	Sun gear
Stage 2 input:	Planet Carrier
Stage 1 output:	Planet Carrier
Stage 2 output:	Sun gear

Peripheral Characteristic	Input Shaft	Output Shaft	Connecting Shaft
Inertia (in-lb-s^2)	2.5	1.0	-
Stiffness (in-lb/rad)	1.0×10^5	1.8×10^7	3.9×10^9

Planetary Gear Characteristic	Sun Gear	Planet Gears	Ring Gear	Carrier
Number of Teeth	27	35	99	-
Diametral Pitch*	8.8571	8.8571	9.14286	-
Pressure Angle* (degrees)	24.6	24.6	20.19	-
Root Radius (in)	1.39	1.802	5.594	-
Tooth Tip Radius (in)	1.655	2.067	5.35	-
Face Width (in)	1.375	1.20	1.00	-
Inertia (in-lb-s^2)	0.026	0.016	0.0	0.20

Note* The variation in diametral pitch and pressure angle cannot be accurately modeled, as the program assumes equal pressure angles at the sun-planet and ring-planet meshes.

Table 3: Two Stage Test Case Parameter Variations

CASE NUMBER	ATTACHED INERTIAS (in-lbs-s²)		SHAFT STIFFNESSES (in-lb/rad)		
	INPUT	OUTPUT	INPUT	OUTPUT	CONNECTING
1	10	15	10	10	10
2	100	10	10	10	10
3	15	10	10	10	10
4	10	10	10	10	$1x10^9$
5	10	10	0	10	10
6	10	10	10	10	$1x10^5$
7	10	10	$1x10^6$	10	10

Table 4: Results of Two Stage Test Case Parametric Variations

CASE NUMBER	STAGE	DISPLACEMENTS, IN.				
		INPUT SHAFT $x10^2$	OUTPUT SHAFT $x10^2$	SUN GEAR $x10^4$	CARRIER $x10^5$	PLANET $x10^4$
1	1	.8017	-	.6941	.7872	.2067
	2	-	.5345	.4274	.503	.1292
2	1	.08018	-	.06955	.07985	.02071
	2	-	.8018	.6408	.7528	.1937
3	1	.5345	-	.463	.526	.1379
	2	-	.8018	.6408	.7534	.1937
4	1	.8003	-	.6899	.7629	.2051
	2	-	.8003	.639	.7629	.1928
5	1	.8004	-	.616E-4	.1095E-2	.1974E-4
	2	-	.8004	.638	.7466	.1925
6	1	.8017	-	.6935	.777	.2065
	2	-	.8017	.6414	.764	.1938
7	1	19.889	-	2755.6	9612	1247.9
	2	-	13.364	59.4	231.8	26.1

NOTE: These displacements are at the end of the first boundary condition iteration.

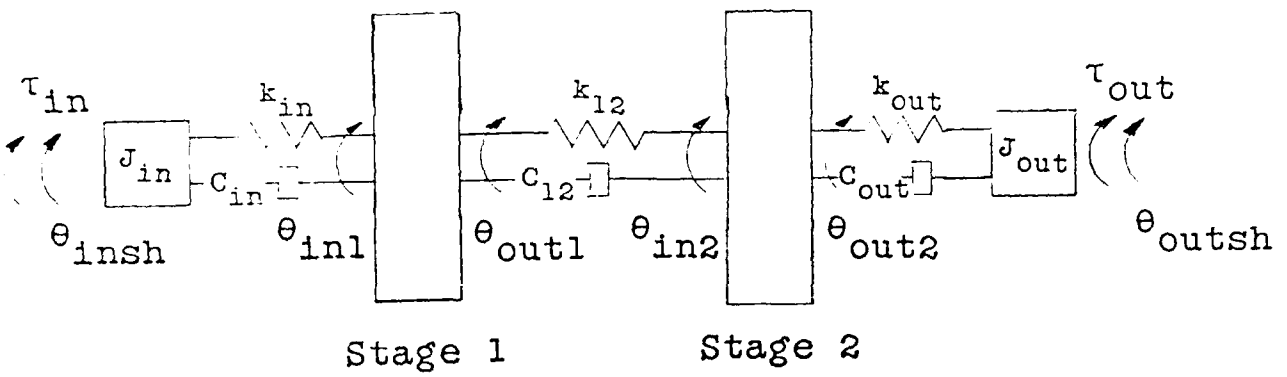

Figure 1: Two Stage System Diagram

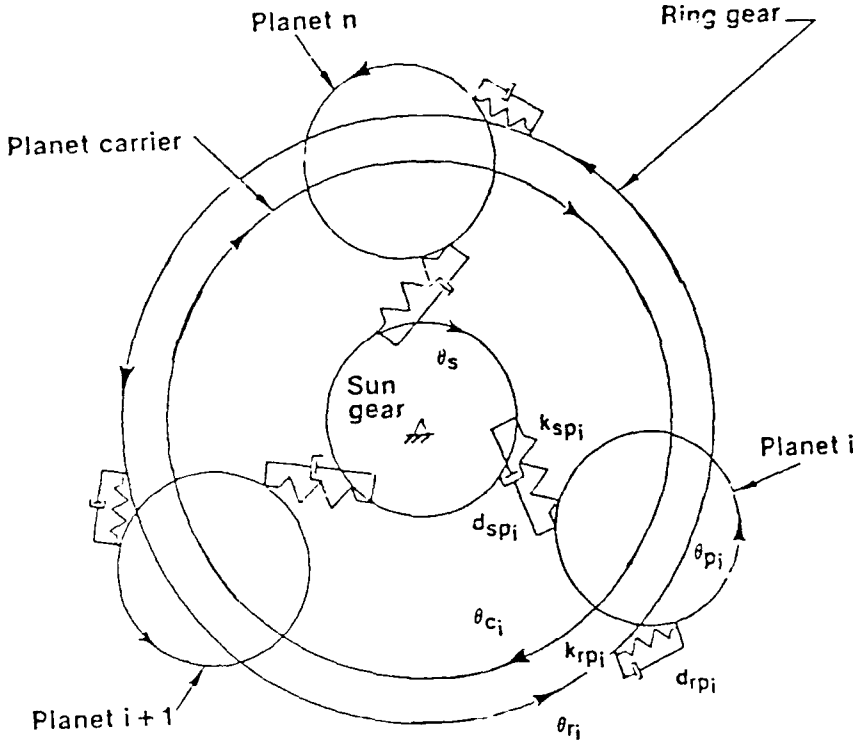

Figure 2: Dynamic Model for Epicyclic Gear Stage

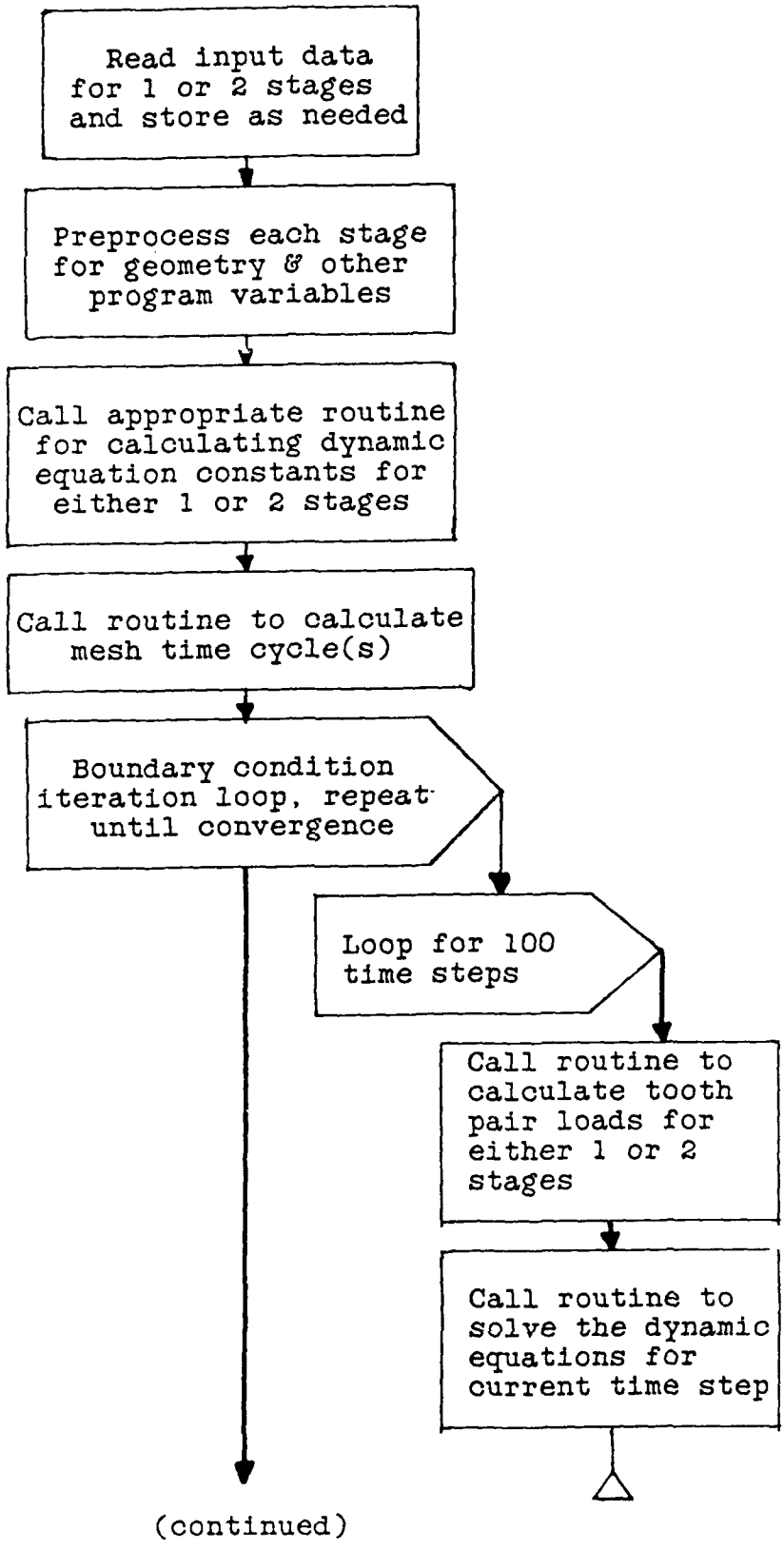

Figure 3: General Program Flowchart

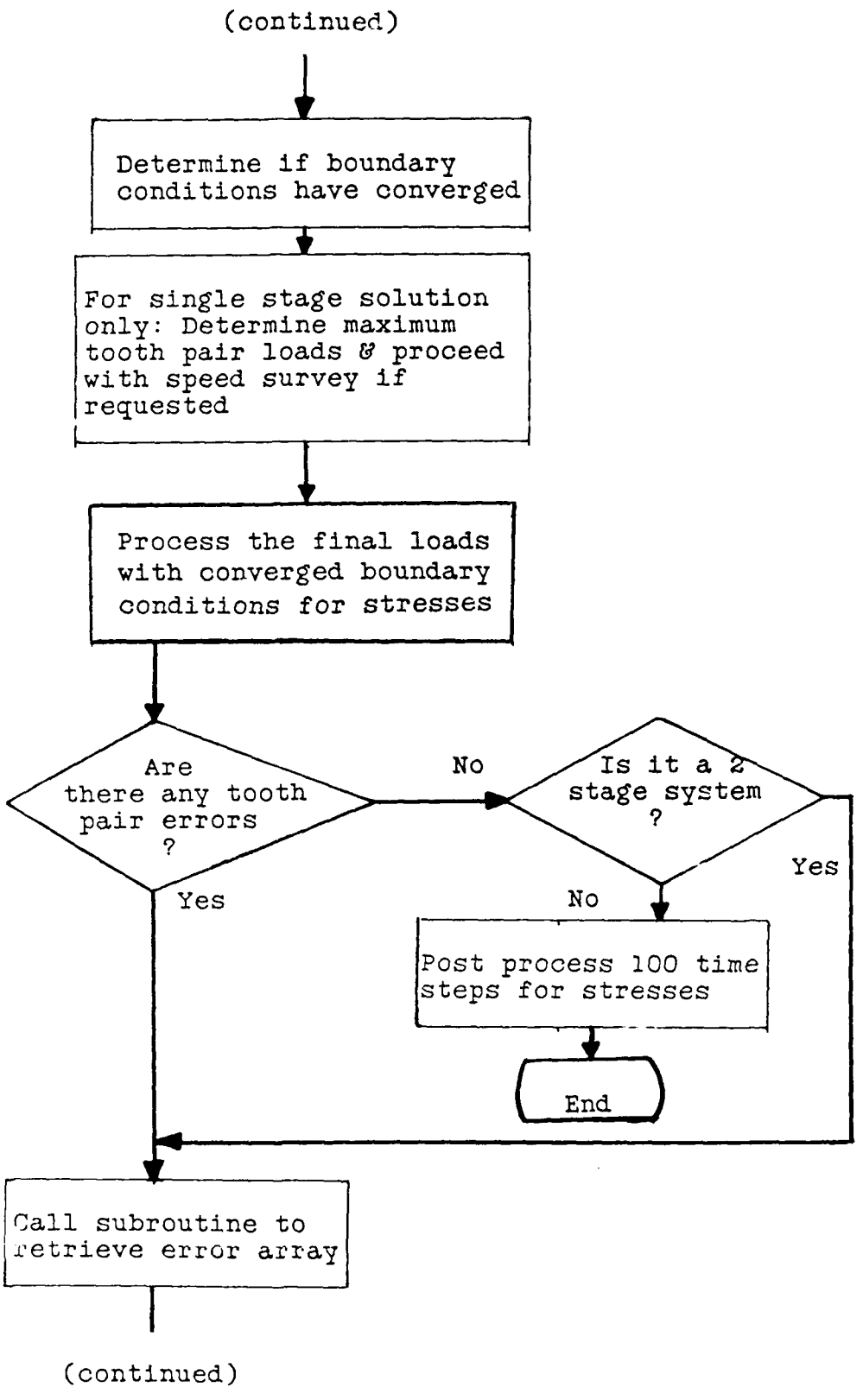

Figure 3: General Program Flowchart (continued)

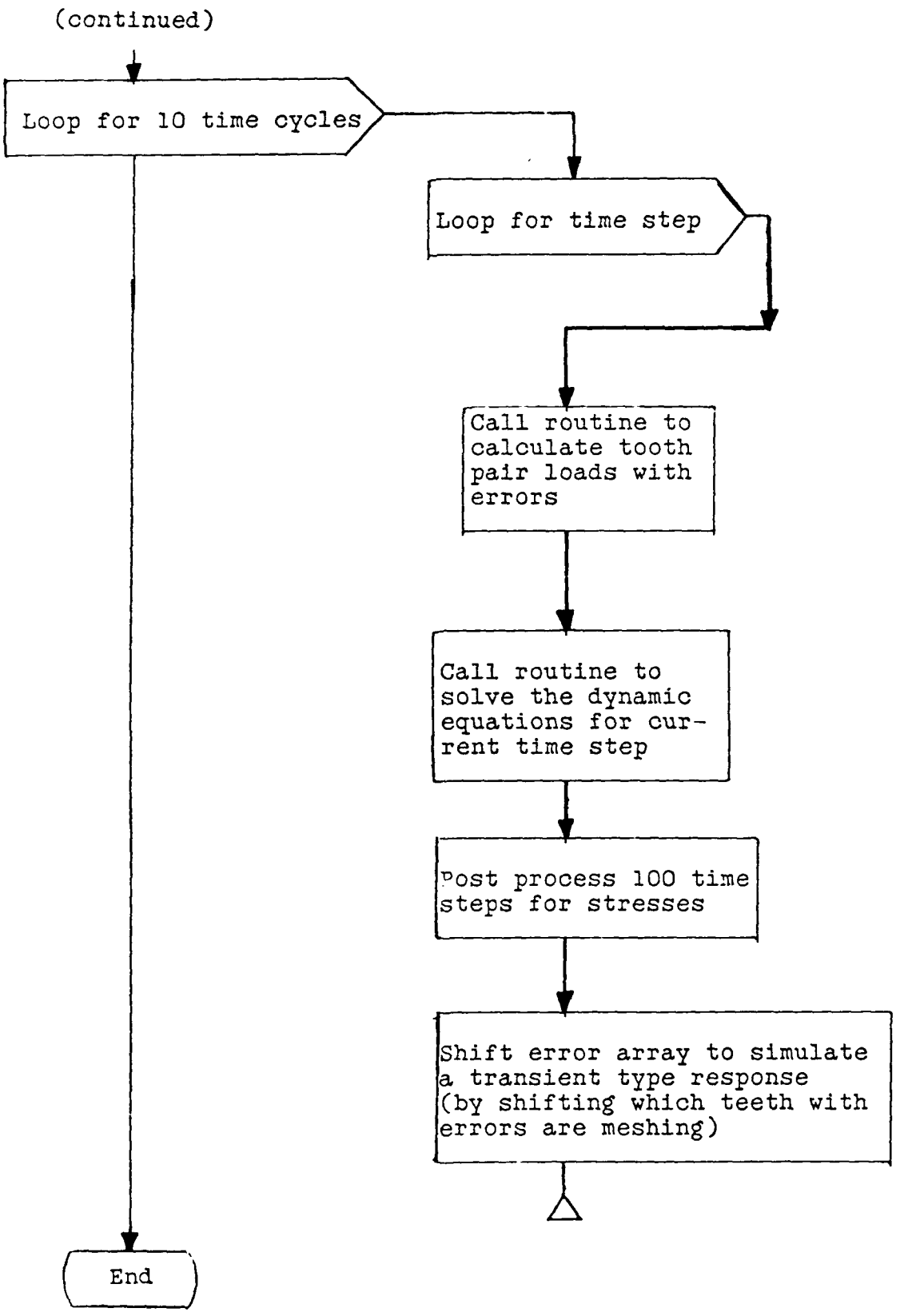

Figure 3: General Program Flowchart (continued)

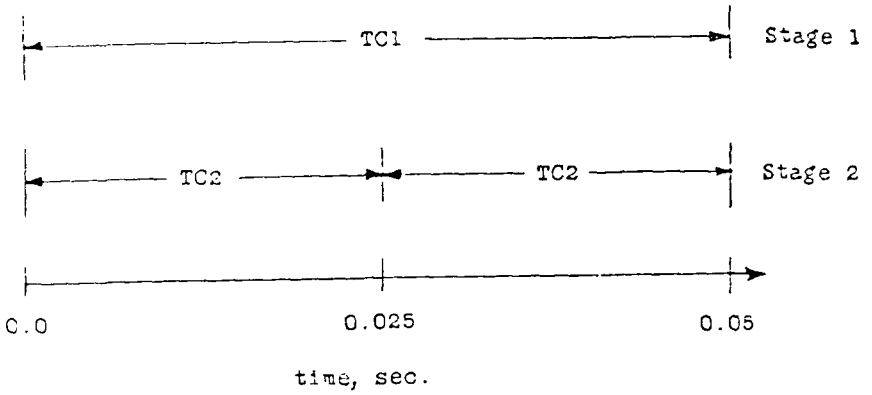

TC1/TC2 = 0.05/0.025 = 2.0

Number of Boundary Condition Cycles for Steady State = 2

TC1 = Time Cycle for stage 1

TC2 = Time Cycle for stage 2

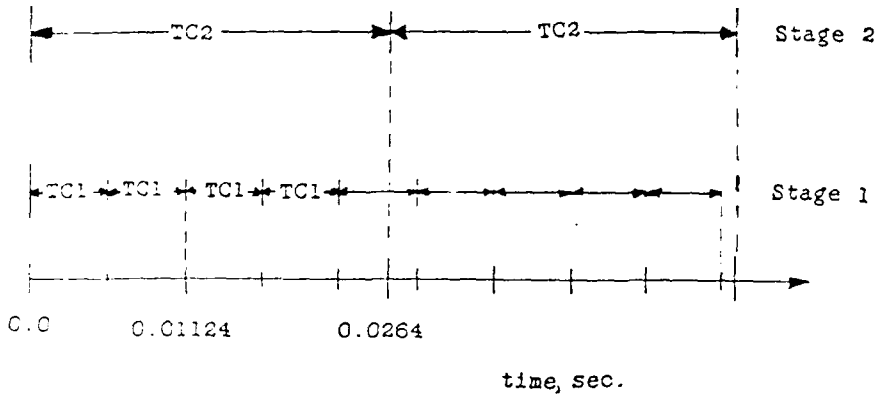

TC2/TC1 = 0.0264/.00562 = 4.7

10 x TC2 = 0.264 sec.

47 x TC1 = 0.264 sec.

Number of Boundary Condition Cycles for Steady State = 47

Figure 4: Two Stage Time Cycle/Boundary Condition Diagram

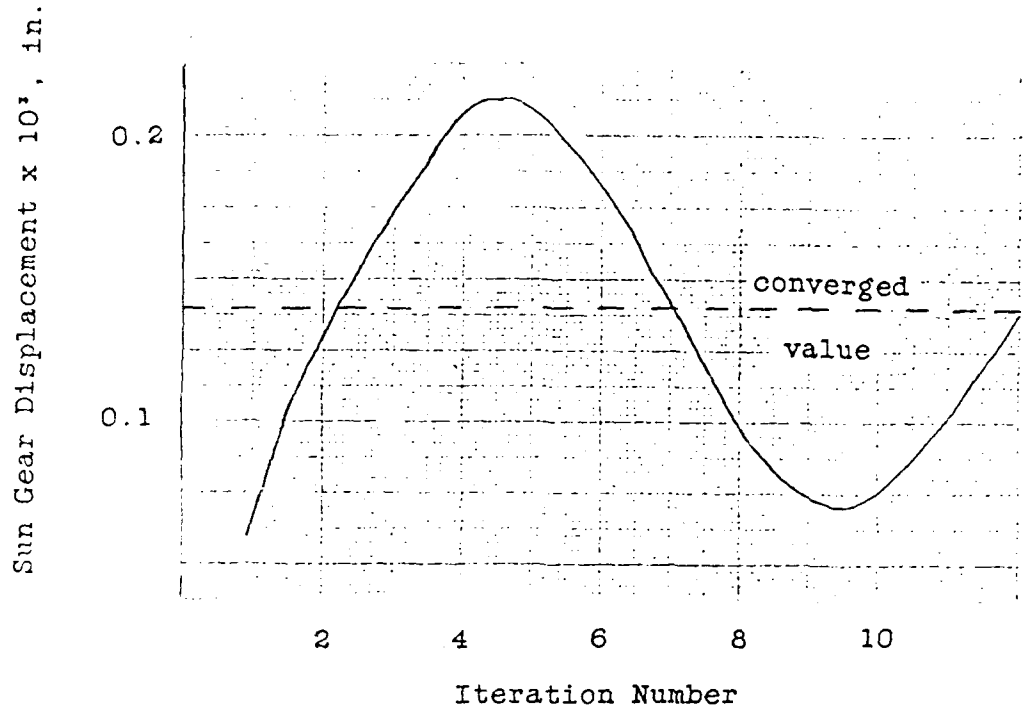

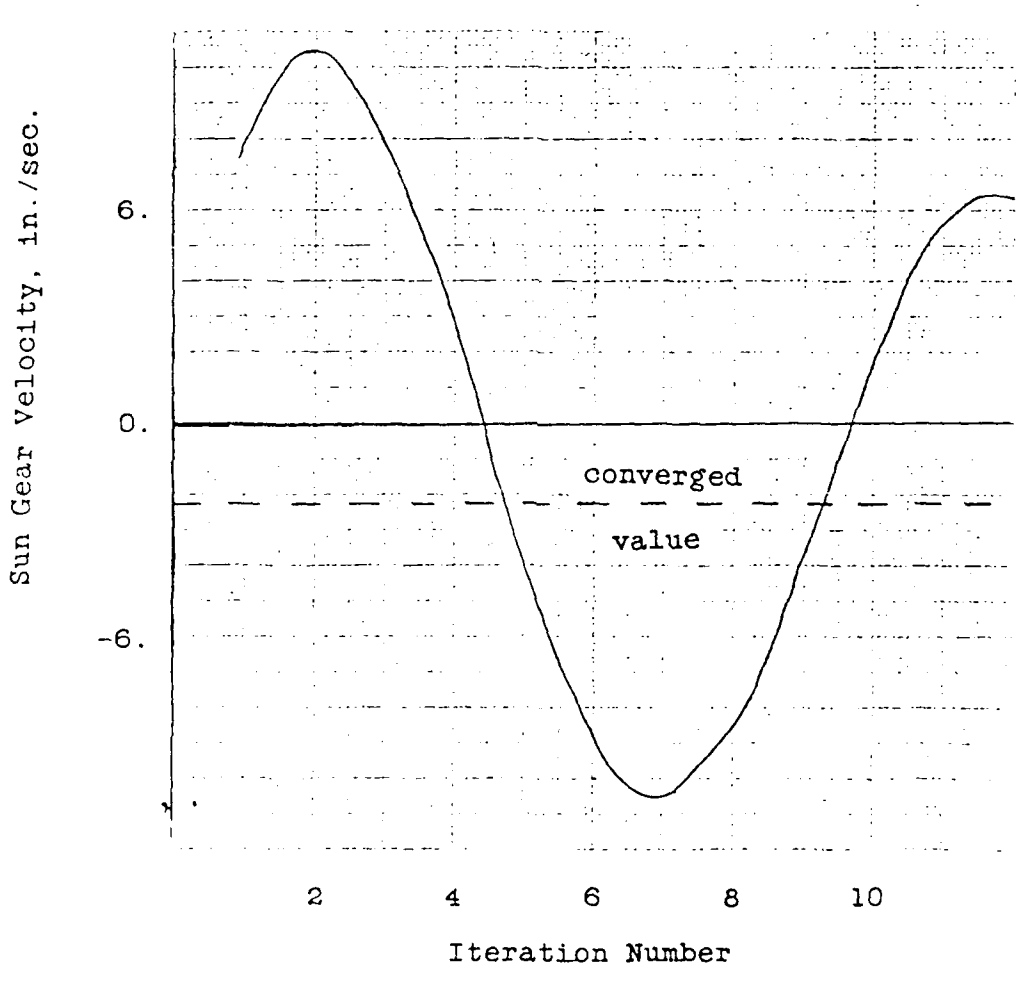

Figure 5: Sun Gear Displacement and Velocity Boundary Conditions vs. Number of Iterations

Original Code

```
621   X = .5*(XS0 + SXS0)
      SXS0 = XS0
      XS0 = X
      X = .5*(XS1 + SXS1)
      SXS1 = XS1
      XS1 = X
      DO 622 IP=1,N
      X = .5*(XP0(IP) + SXP0(IP))
      SXP0(IP) = XP0(IP)
      XP0(IP) = X
      X = .5*(XC0(IP) + SXC0(IP))
      SXC0(IP) = XC0(IP)
      XC0(IP) = X
      X = .5*(XR0(IP) + SXR0(IP))
      SXR0(IP) = XR0(IP)
      XR0(IP) = X
      X = .5*(XP1(IP) + SXP1(IP))
      SXP1(IP) = XP1(IP)
      XP1(IP) = X
      X = .5*(XC1(IP) + SXC1(IP))
      SXC1(IP) = XC1(IP)
      XC1(IP) = X
      X = .5*(XR1(IP) + SXR1(IP))
      SXR1(IP) = XR1(IP)
622   XR1(IP) = X
```

Recommended Code Revisions

Weighting Coefficients: Displacement → .70, .30; Velocity → .50, .50

```
621   X = .5*(XS0 + SXS0)
      SXS0 = .70*SXS0 + .30* XS0
      XS0 = X
      X = .5*(XS1 + SXS1)
      SXS1 = .50*SXS1 + .50*XS1
      XS1 = X
      DO 622 IP=1,N
      X = .5*(XP0(IP) + SXP0(IP))
      SXP0(IP) = .70*SXP0(IP) + .30*XP0(IP)
      XP0(IP) = X
      X = .5*(XC0(IP) + SXC0(IP))
      SXC0(IP) = .70*SXC0(IP) + .30*XC0(IP)
      XC0(IP) = X
      X = .5*(XR0(IP) + SXR0(IP))
      SXR0(IP) = .70*SXR0(IP) + .30*XR0(IP)
      XR0(IP) = X
      X = .5*(XP1(IP) + SXP1(IP))
      SXP1(IP) = .50*SXP1(IP) + .50*XP1(IP)
      XP1(IP) = X
      X = .5*(XC1(IP) + SXC1(IP))
      SXC1(IP) = .50*SXC1(IP) + .50*XC1(IP)
      XC1(IP) = X
      X = .5*(XR1(IP) + SXR1(IP))
      SXR1(IP) = .50*SXR1(IP) + .50*XR1(IP)
622   XR1(IP) = X
```

Figure 6: Code Revisions to Weight Previous Boundary Condition Iterations

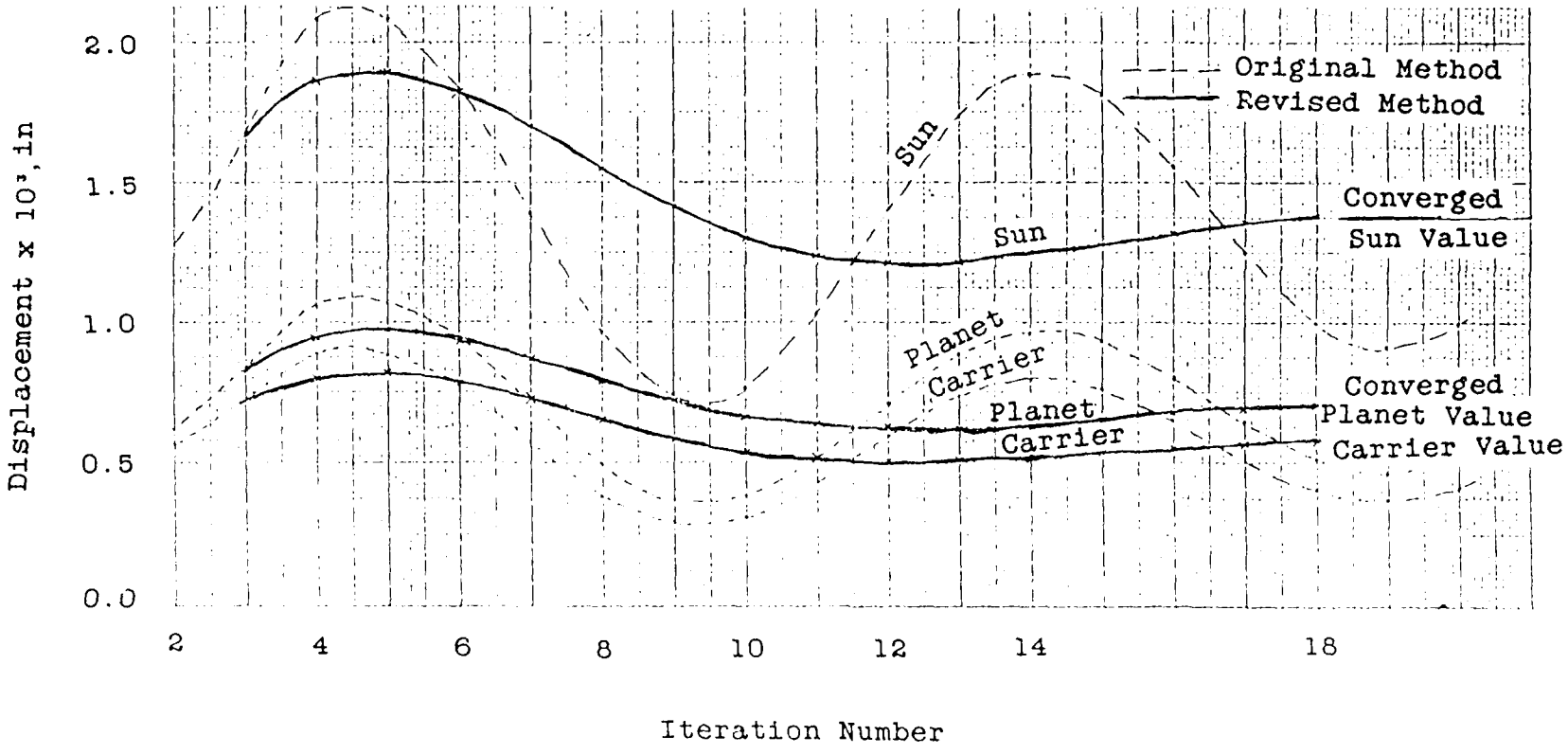

Figure 7: Displacement Boundary Conditions vs. Number of Iterations

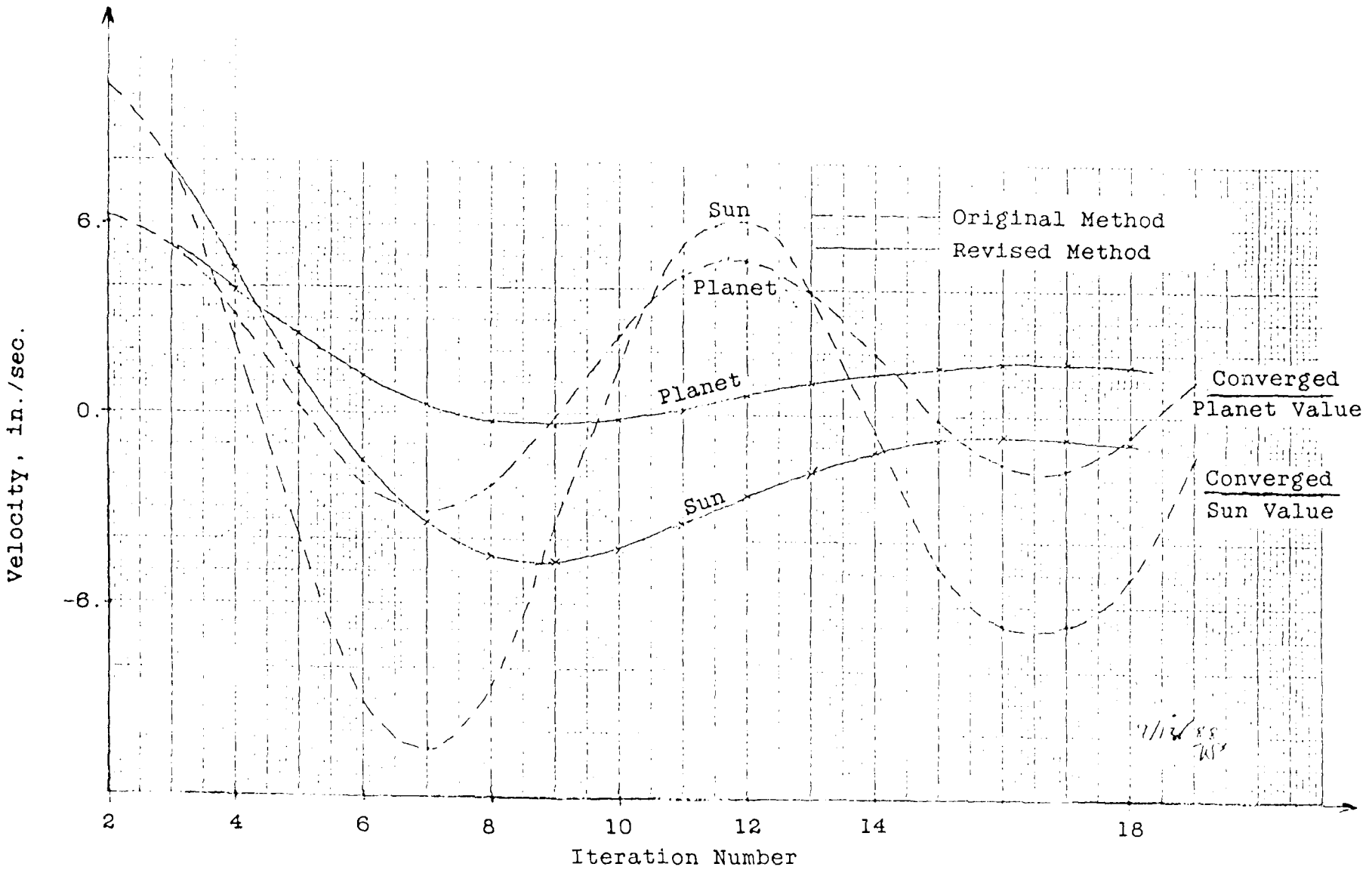

Figure 8: Velocity Boundary Conditions vs. Number of Iterations

```
SINGLE STAGE CHECK CASE, OH-58
1          1.          1.
2          2.       8.8571        24.6
3          6.          27.          35.         99.
5          9.       1.375           1.          1.         3.0          1.
4         14.        5000.         500.        500.         1.0
5         28.        .026         .2000         .00        .0160         .016
5         33.        .016
2        150.         .01          20.
1        651.          1.
0-1.
```

Figure 9a: Single Stage OH-58 Test Case Input

INPUT DATA

NO.TEETH - SUN	27.0000
NO.TEETH - PLANET	35.0000
PRESSURE ANGLE (DEGREES) DRIVE SIDE	24.6000
DIAMETRAL PITCH	8.8571
TOOTH TIP RADIUS TOL. (INCH)	0.0020
EDGE BREAK ON TOPLAND (INCH)	0.0100
MACHINED BACKLASH TOL.(INCH)	0.0020
ROOT RADIUS TOL. (INCH)	0.0050
FACE WIDTH - SUN (INCH)	1.3750
FACE WIDTH - PLANET (INCH)	1.2000
YOUNGS MOD.*E-6 - SUN (LB/SQ.INCH)	30.0000
YOUNGS MOD.*E-6 - PLANET (LB/SQ.INCH)	30.0000
POISSONS RATIO - SUN	0.3000
POISSONS RATIO - PLANET	0.3000
SURFACE ROUGHNESS-MAX (AA)	25.0000
OIL INLET TEMPERATURE (DEG.F)	180.0000
INITIAL RPM OF RANGE	500.0000
FINAL RPM OF RANGE	500.0000
NUMBER OF INTERVALS	1.0000
TORQUE INPUT (IN-LBS)	5000.0000
TOTAL INV.PROFILE MODIFICATION,ENGAGE (INCH)	0.0000
TOTAL INV.PROFILE MODIFICATION,DISENG (INCH)	0.0000
INV.PROFILE MOD.LOCATION-% OF SOE	0.0000
INV.PROFILE MOD.LOCATION-% OF SOD	0.0000
INV.PROFILE MOD.TOTAL TOLERANCE	0.0000
+C.D.TOL. (OUT OF MESH) (INCH)	0.0000
-C.D.TOL. (INTO MESH) (INCH)	0.0000
CONTACT RATIO INPUT	0.0000
HERTZ CONSTANT FOR COMPLIANCE	209862.
CENTER DISTANCE,THEO. (INCH)	3.5000
CENTER DISTANCE,MAX. (INCH)	3.5000
CENTER DISTANCE,MIN. (INCH)	3.5000
CIRCULAR PITCH (INCH)	0.3547
CIRCULAR BASE PITCH (INCH)	0.3225
MAX.OPERATING PRESS. ANGLE (DEG) DRIVE	24.6000
MIN.OPERATING PRESS. ANGLE (DEG) DRIVE	24.6000
NOMINAL CONTACT RATIO AT C.D.-THEO.	1.4867
MINIMUM CONTACT RATIO AT C.D.-MAX.	1.3426
MATERIAL CONSTANT	0.0528
CODE FOR TYPE OF OIL	0.0000

		SUN	PLANET
NUMBER OF TEETH		27.0000	35.0000
PITCH DIAMETER	(INCH)	3.0484	3.9516
BASE CIRCLE DIA. DRIVE SIDE	(INCH)	2.7717	3.5930
TOOTH TIP DIAMETER,MAX.	(INCH)	3.2862	4.1654
TOOTH TIP DIAMETER,MIN.	(INCH)	3.2822	4.1614
EFFECTIVE TOOTH TIP DIA	(INCH)	3.2622	4.1414
ROOT DIAMETER,MAX.	(INCH)	2.8089	3.6945
ROOT DIAMETER,MIN.	(INCH)	2.7989	3.6845
TRUE INV.FORM DIA.	(INCH)	2.8867	3.7721
TOPLAND WIDTH,MIN.	(INCH)	0.0586	0.0636
ROOT FILLET RADIUS,MIN.	(INCH)	0.0489	0.0508
MACHINE BACKLASH,MAX.	(INCH)	0.0025	0.0025
MACHINE BACKLASH,MIN.	(INCH)	0.0005	0.0005
CIRCULAR TOOTH THICKNESS	(INCH)	0.1828	0.1719
MACH.CIRC.TOOTH THKNS.MAX.	(INCH)	0.1823	0.1714
MACH.CIRC.TOOTH THKNS.MIN.	(INCH)	0.1803	0.1694
TIP/ROOT CLEAR.MIN AT CD MIN.	(INCH)	0.0128	0.0097
ROLL ANGLE AT TOOTH TIP DIA.	(DEG)	36.4943	33.6071
ROLL ANGLE	(DEG)	26.2319	26.2319
AT ADD.INV.MODIFICATION DIA.	(INCH)	3.0484	3.9516
ROLL ANGLE AT PITCH DIA.	(DEG)	26.2319	26.2319
ROLL ANGLE	(DEG)	26.2319	26.2319
AT DED.INV.MODIFICATION DIA.	(INCH)	3.0484	3.9516
ROLL ANGLE AT TIED	(DEG)	16.6714	18.3154
INSPECTION WIRE/BALL DIA.	(INCH)	0.1950	0.2100
MAX.MEASUREMENT OVER 2 WIRE/BALL	(INCH)	3.3245	4.2561
MIN.MEASUREMENT OVER 2 WIRE/BALL	(INCH)	3.3207	4.2521
EFFECTIVE WIDTH AT TOOTH TIP		1.3750	1.2000
EFFECTIVE WIDTH AT START OF FILLET		1.3750	1.2000
RADIUS TO BASE OF FILLET INPUT (INCH)		0.0000	0.0000
OUTSIDE RADIUS INPUT (INCH)		0.0000	0.0000
FILLET RADIUS INPUT (INCH)		0.0000	0.0000
DAMPING RATIO INPUT		0.0000	0.0000

Figure 9b: Single Stage OH-58 Output Summary for Preprocessed Geometry

INPUT DATA

NO.TEETH - PLANET(EXTERNAL GEAR)	35.0000
NO.TEETH - RING (INTERNAL GEAR)	99.0000
PRESSURE ANGLE (DEGREES) DRIVE SIDE	24.6000
DIAMETRAL PITCH	8.8571
TOOTH TIP RADIUS TOL. (INCH)	0.0020
EDGE BREAK ON TOPLAND (INCH)	0.0100
MACHINED BACKLASH TOL.(INCH)	0.0020
ROOT RADIUS TOL. (INCH)	0.0050
FACE WIDTH - PLANET (INCH)	1.2000
FACE WIDTH - RING (INCH)	1.0000
YOUNGS MOD.*E-6 - PLANET (LB/SQ.INCH)	30.0000
YOUNGS MOD.*E-6 - RING (LB/SQ.INCH)	30.0000
POISSONS RATIO - PLANET	0.3000
POISSONS RATIO - RING	0.3000
SURFACE ROUGHNESS-MAX (AA)	25.0000
OIL INLET TEMPERATURE (DEG.F)	180.0000
INITIAL RPM OF RANGE	500.0000
FINAL RPM OF RANGE	500.0000
NUMBER OF INTERVALS	1.0000
TORQUE INPUT (IN-LBS)	5000.0000
TOTAL INV.PROFILE MODIFICATION,ENGAGE (INCH)	0.0000
TOTAL INV.PROFILE MODIFICATION,DISENG (INCH)	0.0000
INV.PROFILE MOD.LOCATION-% OF SOE	0.0000
INV.PROFILE MOD.LOCATION-% OF SOD	0.0000
INV.PROFILE MOD.TOTAL TOLERANCE	0.0000
+C.D.TOL. (OUT OF MESH) (INCH)	0.0000
-C.D.TOL. (INTO MESH) (INCH)	0.0000
CONTACT RATIO INPUT	0.0000
HERTZ CONSTANT FOR COMPLIANCE	155022.
CENTER DISTANCE,THEO. (INCH)	3.6129
CENTER DISTANCE,MAX. (INCH)	3.6129
CENTER DISTANCE,MIN. (INCH)	3.6129
CIRCULAR PITCH (INCH)	0.3547
CIRCULAR BASE PITCH (INCH)	0.3225
MAX.OPERATING PRESS. ANGLE (DEG) DRIVE	24.6000
MIN.OPERATING PRESS. ANGLE (DEG) DRIVE	24.6000
NOMINAL CONTACT RATIO AT C.D.-THEO.	1.6407
MINIMUM CONTACT RATIO AT C.D.-MAX.	1.4680
MATERIAL CONSTANT	0.0528
CODE FOR TYPE OF OIL	0.0000

		PLANET	RING
NUMBER OF TEETH		35.0000	99.0000
PITCH DIAMETER	(INCH)	3.9516	11.1775
BASE CIRCLE DIA. DRIVE SIDE	(INCH)	3.5930	10.1630
TOOTH TIP DIAMETER,MAX.	(INCH)	4.1774	10.9557
TOOTH TIP DIAMETER,MIN.	(INCH)	4.1734	10.9517
EFFECTIVE TOOTH TIP DIA	(INCH)	4.1534	10.9757
ROOT DIAMETER,MAX.	(INCH)	3.6790	11.4377
ROOT DIAMETER,MIN.	(INCH)	3.6690	11.4277
TRUE INV.FORM DIA.	(INCH)	3.7497	11.3884
TOPLAND WIDTH,MIN.	(INCH)	0.0630	0.0757
ROOT FILLET RADIUS,MIN.	(INCH)	0.0446	0.0399
MACHINE BACKLASH,MAX.	(INCH)	0.0025	0.0025
MACHINE BACKLASH,MIN.	(INCH)	0.0005	0.0005
CIRCULAR TOOTH THICKNESS	(INCH)	0.1773	0.1773
MACH.CIRC.TOOTH THKNS.MAX.	(INCH)	0.1773	0.1773
MACH.CIRC.TOOTH THKNS.MIN.	(INCH)	0.1753	0.1753
TIP/ROOT CLEAR.MIN AT CD MIN.	(INCH)	0.0234	0.0122
ROLL ANGLE AT TOOTH TIP DIA.	(DEG)	33.9839	23.0065
ROLL ANGLE	(DEG)	26.2319	26.2318
AT ADD.INV.MODIFICATION DIA.	(INCH)	3.9516	11.1775
ROLL ANGLE AT PITCH DIA.	(DEG)	26.2319	26.2319
ROLL ANGLE	(DEG)	26.2319	26.2318
AT DED.INV.MODIFICATION DIA.	(INCH)	3.9516	11.1775
ROLL ANGLE AT TIFD	(DEG)	17.1080	28.9724
INSPECTION WIRE/BALL DIA.	(INCH)	0.2000	0.1950
MAX.MEASUREMENT OVER 2 WIRE/BALL	(INCH)	4.2362	10.8986
MIN.MEASUREMENT OVER 2 WIRE/BALL	(INCH)	4.2322	10.9031
EFFECTIVE WIDTH AT TOOTH TIP		1.2000	1.0000
EFFECTIVE WIDTH AT START OF FILLET		1.2000	1.0000
RADIUS TO BASE OF FILLET INPUT (INCH)		0.0000	0.0000
OUTSIDE RADIUS INPUT (INCH)		0.0000	0.0000
FILLET RADIUS INPUT (INCH)		0.0000	0.0000
DAMPING RATIO INPUT		0.0000	0.0000

Figure 9b: Single Stage CH-58 Output Summary for Preprocessed Geometry (continued)

NUMBER OF PLANETS	3
NUMBER OF BOUNDARY CONDITION ITERATIONS	20
TOLERANCE FOR BOUNDARY CONDITION CONVERGENCE	0.10000E-01

EQUIVALENT MASS OF SUN GEAR	0.26000E-01
EQUIVALENT MASS OF PLANET CARRIER	0.20000E+00
EQUIVALENT MASS OF RING GEAR	0.00000E+00
EQUIVALENT MASS OF PLANET # 1	0.16000E-01

COMPLIANCE CONSTANTS

SUN-PLANET

0.2842E-06 * (1 + -0.7912E-01 * (S/SO) + 0.3962E+00 * (S/SO)**2 + -0.3896E-01 * (S/SO)**3 + 0.1945E+00 * (S/SO)**4)

RING-PLANET

0.2976E-06 * (1 + -0.1303E+00 * (S/SO) + 0.1867E+00 * (S/SO)**2 + 0.1419E+00 * (S/SO)**3 + 0.2547E+00 * (S/SO)**4)

********** PLANETARY GEAR SYSTEM **********

THE MESH CYCLE TIME IS = 0.566E-02 SECONDS

NO TOOTH ERRORS SOLUTION

MAXIMUM VALUES FOR SUN-PLANET MESH 1

	SUN		PLANET
FILLET STRESS CONCENTRATION (KSUBT)	1.51556		1.49935
MAXIMUM HERTZ STRESS	139168.1		139168.1
MAXIMUM HERTZ STRESS AT PD	101771.9		101771.9
MAXIMUM BENDING STRESS	18130.2		26327.1
MAXIMUM BENDING STRESS AT PD	10387.1		12060.0
DEPTH TO MAXIMUM SHEAR	0.00458		0.00458
MAXIMUM DYNAMIC PV(MILLIONS OF PSI*FT/MIN)	10.92694		10.92694
MAXIMUM FLASH TEMPERATURE		220.7	
MAXIMUM NORMAL LOAD		1760.2	
AVERAGE COEFFICIENT OF FRICTION		0.13994	
RPM FOR STRESSES		500.00	

* *
THE EFFECTIVE CONTACT RATIO = 1.4800
* *

MAXIMUM VALUES FOR RING-PLANET MESH 1

	PLANET		RING
FILLET STRESS CONCENTRATION (KSUBT)	1.54924		1.63515
MAXIMUM HERTZ STRESS	121815.7		121815.7
MAXIMUM HERTZ STRESS AT PD	50787.4		50787.4
MAXIMUM BENDING STRESS	23459.7		27738.4
MAXIMUM BENDING STRESS AT PD	8224.9		2365.9
DEPTH TO MAXIMUM SHEAR	0.00667		0.00667
MAXIMUM DYNAMIC PV(MILLIONS OF PSI*FT/MIN)	4.22518		4.22518
MAXIMUM FLASH TEMPERATURE		195.8	
MAXIMUM NORMAL LOAD		1935.5	
AVERAGE COEFFICIENT OF FRICTION		0.07535	
RPM FOR STRESSES		500.00	

* *
THE EFFECTIVE CONTACT RATIO = 1.6400
* *

Figure 9b: Single Stage OH-58 Output Summary for Preprocessed Geometry (continued)

```
PLANETARY GEAR, SIMILAR TO THE OH-58 BACK-TO-BACK TEST RIG SETUP
1          1.          1.
2          2.       8.8571       24.6
3          6.         27.         35.         99.
5          9.        1.375        1.2          1.         3.0          1.
4         14.         5000.       500.        500.        1.0
5         28.          .026       .2500        .25        .0160        .016
5         33.          .016
2        150.          .80          5.
1        651.          0.
5        810.          1.          1.E1        1.E1        1.E1        0.14
4        815.          .13         .15         10.         15.
1        827.          5.
0        819.        0.0000      .000000     00.00000     .000000
0        823.     .0000000       00.0000    .00000000     00.000
0        830.      .000000       .000000      .00000
0        840.    .00000000     .00000000    .00000000
0        850.     00.00000      00.00000     00.00000
0        860.     0.000000      0.000000     0.000000
0        561.     .0000000
0        581.     00.00000
0        571.     .0000000
0        591.     0.000000
1       1001.          1.
2       1002.       8.8571       24.6
3       1006.         27.         35.         99.
5       1009.        1.375        1.2          1.         3.0         -1.
4       1014.        23333.       107.        107.        1.0
5       1028.         .026        .2500        .25        .0160        .016
5       1033.         .016
2       1150.         .80          5.
0-1.
```

Figure 10: Two Stage OH-58 Input Data Set

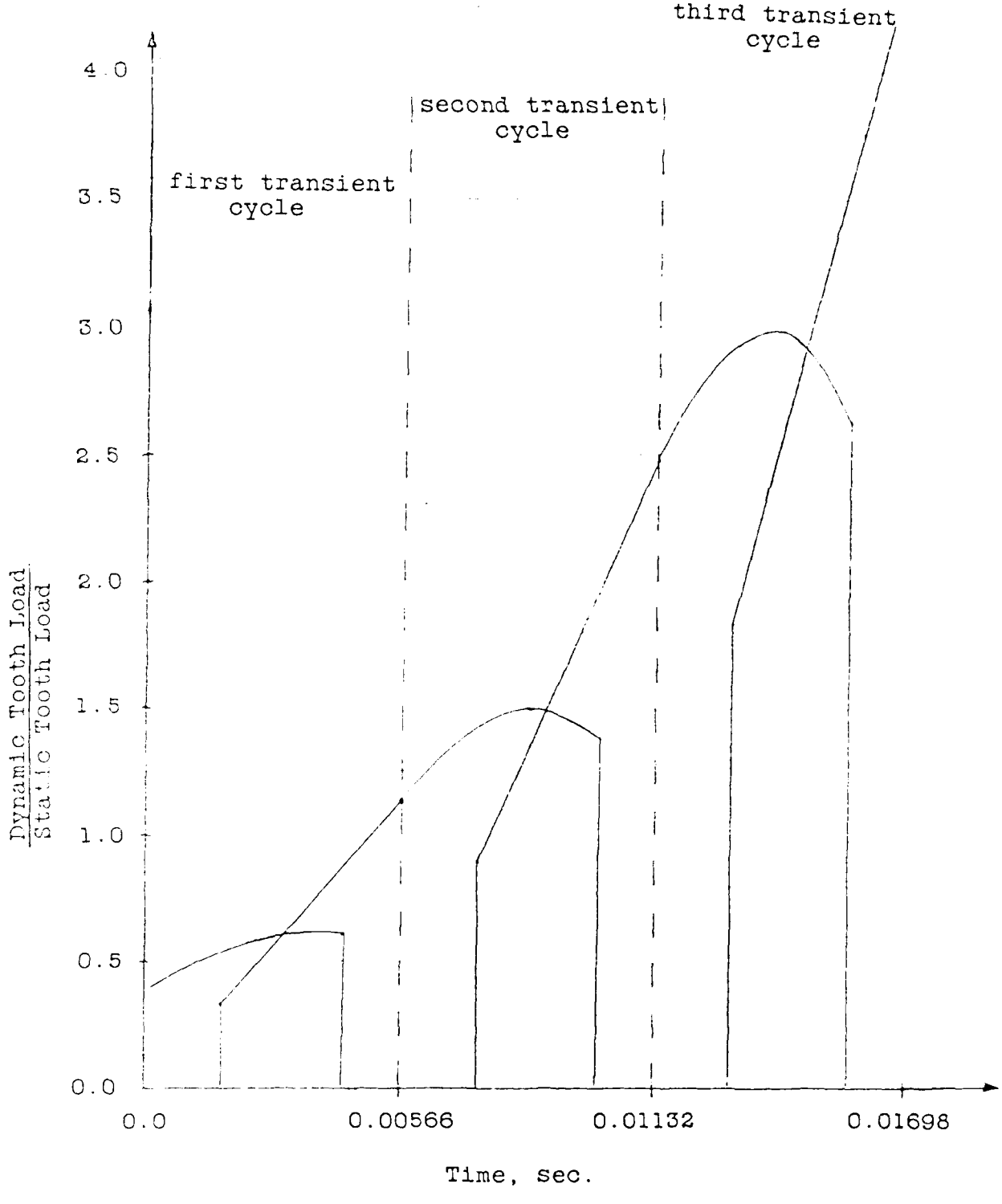

Figure 11a: Dynamic Loads for OH-58 First Stage Sun-Planet Mesh

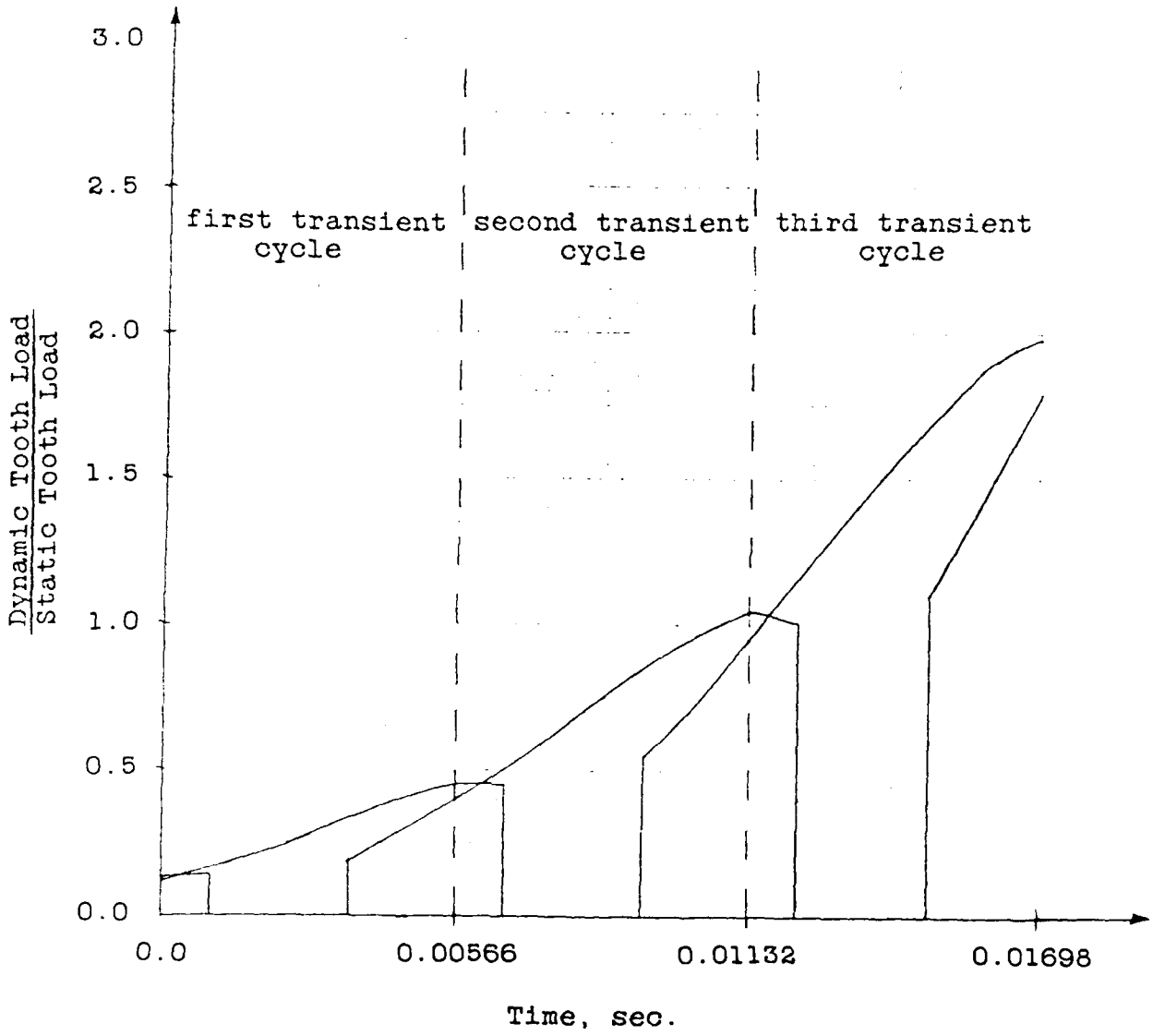

Figure 11b: Dynamic Loads for OH-58 First Stage Ring-Planet Mesh

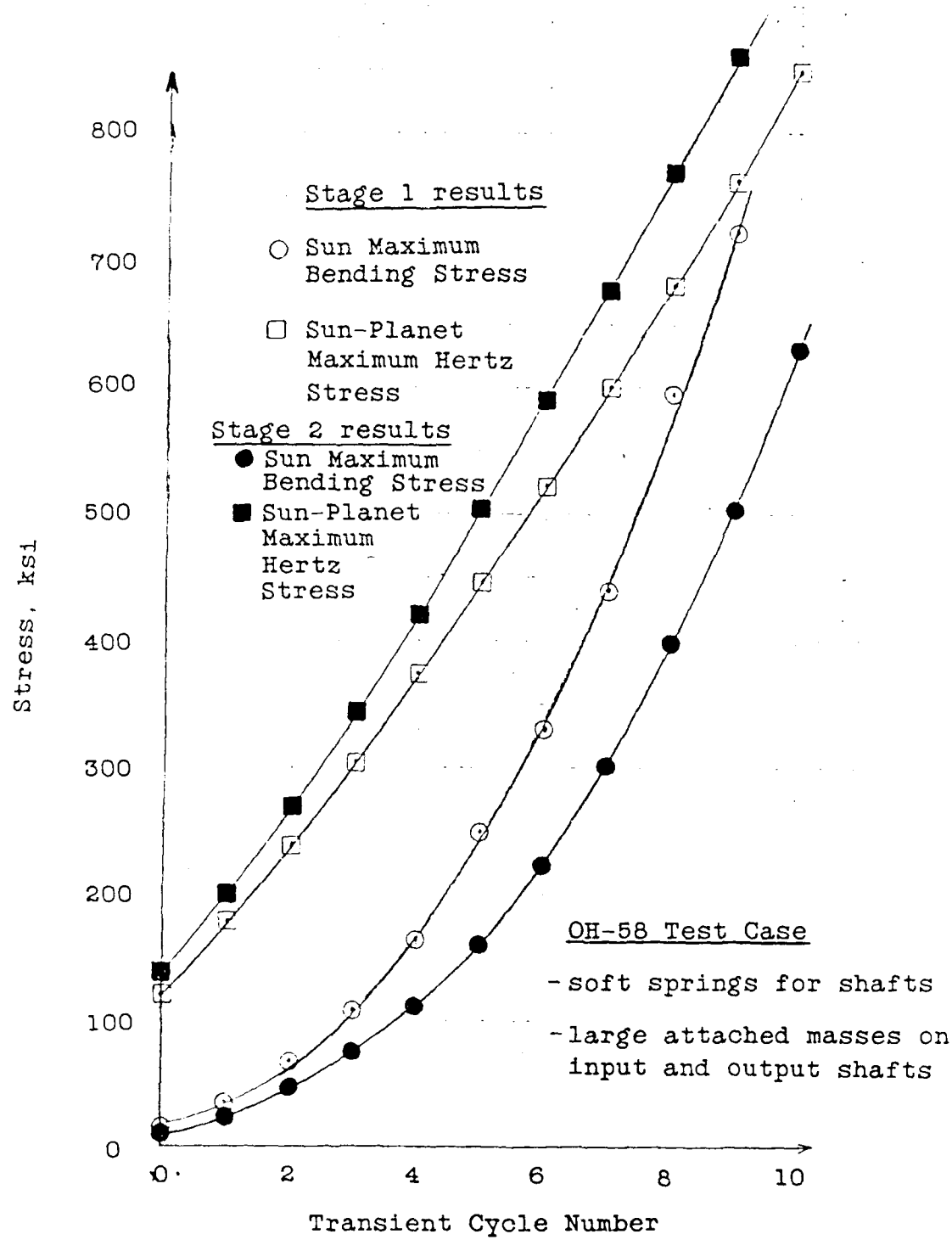

Figure 12: Maximum Stress vs. Transient Cycle Number

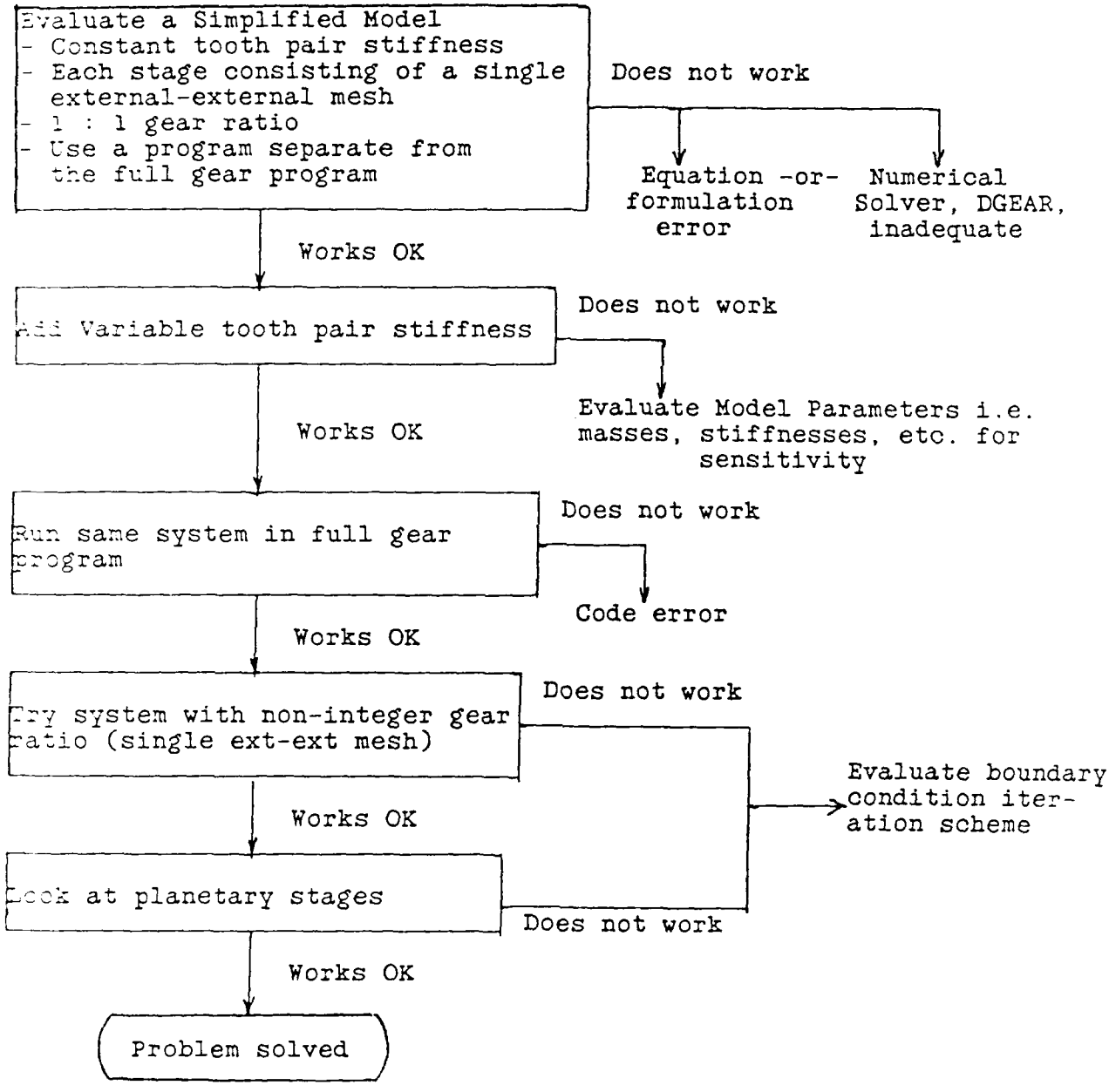

Figure 13: Procedure to Locate Source of Instability

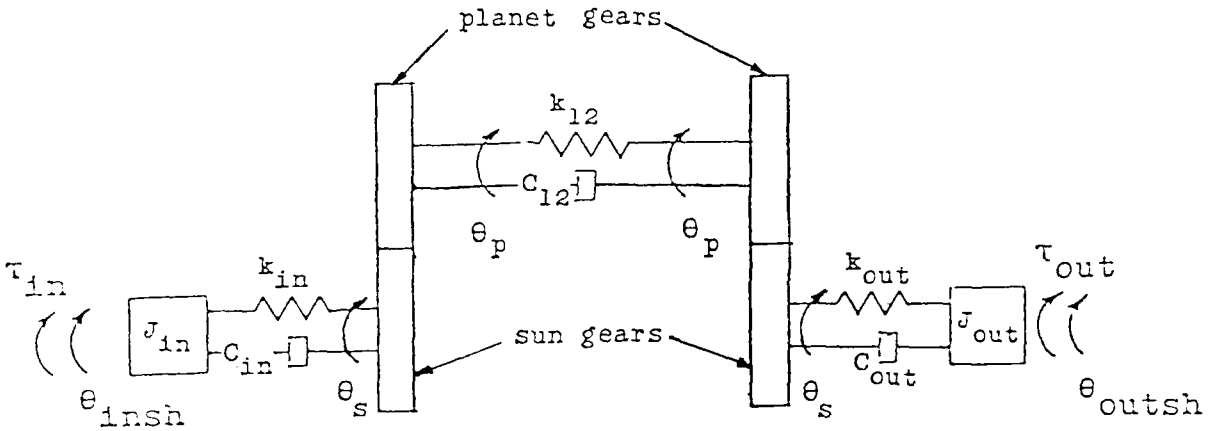

Figure 14: Simple Two Stage System Schematic

NASA

Report Documentation Page

1 Report	Government Accession No.	3. Recipient's Catalog No.
NASA CR-185110 AVSCOM TM 89-C-003		

4 Title and Subtitle	5. Report Date
Two Stage Gear Tooth Dynamics Program	August 1989
	6. Performing Organization Code

7. Author(s)	8. Performing Organization Report No.
Linda S. Boyd	HSER 12648
	10. Work Unit No. 505-63-5A 505-62-0K

9. Performing Organization Name and Address	11. Contract or Grant No.
Hamilton Standard Division United Technologies Corporation Windsor Locks, Connecticut 06096	NAS3-25281

12 Sponsoring Agency Name and Address	13. Type of Report and Period Covered
Propulsion Directorate U.S. Army Aviation Research and Technology Activity—AVSCOM Cleveland, Ohio 44135-3127 and NASA Lewis Research Center Cleveland, Ohio 44135-3191	Contractor Report Final
	14. Sponsoring Agency Code

15 Supplementary Notes

Project Manager, James J. Zakrajsek, Propulsion Systems Division, NASA Lewis Research Center.

16 Abstract

The purpose of this contract was to expand the epicyclic gear dynamics program to add the option of evaluating the tooth pair dynamics for two epicyclic gear stages with peripheral components. This was a practical extension to the program, as multiple gear stages are often used for speed reduction, space, weight, and/or auxiliary units. The option was developed for either stage to be a basic planetary, star, single external-external mesh, or single external-internal mesh. The two stage system allows for modeling of the peripherals with an input mass and shaft, an output mass and shaft, and a connecting shaft. Execution of the initial test case indicated an instability in the solution with the tooth pair loads growing to excessive magnitudes. A procedure to trace the instability is recommended as well as a method of reducing the program's computation time by reducing the number of boundary condition iterations.

17 Key Words (Suggested by Author(s))	18. Distribution Statement
Gear tooth dynamics Gear tooth stresses Two stage dynamics Epicyclic gears	Unclassified – Unlimited Subject Category 37

19 Security Classif. (of this report)	20 Security Classif. (of this page)	21. No of pages	22 Price*
Unclassified	Unclassified		

*For sale by the National Technical Information Service, Springfield, Virginia 22161